Chapter 6

Preparation and characterization of extract loaded SLN

6.1.Introduction

In present study, we have attempted to target *Ficus religiosa L.* loaded SLNs and functionalized using triphenylphosphonium and study its effect on mitochondrial function in the oxidative stress induced diabetes. Changes in mitochondrial function such as mitochondrial morphology, mitochondrial membrane potential, complex-I, II, IV and V activity, intracellular calcium ion concentration and ROS level were studied. Apoptotic markers such as caspase-3, caspase-9 and cytochrome-c were measured by western blotting. Further, measurement of antioxidants enzyme levels and diabetic biomarkers such as blood glucose, plasma insulin and glycated hemoglobin were carried out along with histopathology study.

6.2.Methods

6.2.1. Preparation of SLN

SLNs were prepared by the combined method of hot homogenization and ultrasonication. Lipid was melted and extract was dispersed in the melted lipid phase. Aqueous phase containing surfactant was poured into the lipid phase which was maintained at the same temperature of lipid phase. The melting point of lupeol is

213 -215° C while the melting points of lipids used were around 50 - 70° C. Hence, lupeol will be stable during hot homogenization process. Lipid and its concentration, surfactant and its concentration, homogenization speed and time and sonication intensity and time were optimized in this study. SLN suspension was then allowed to cool to room temperature. Then, formed suspension was sonicated. Lyophilization of formed suspension was done by using lyophilizer (Decibel Digital Technologies, India). Lyophilisation was conducted for 72 hours at - 60° C temperature.

6.2.1.1.Optimization of lipid

Optimization of lipid and its concentration for the study was carried out using two lipids (glyceryl monostearate and compritol ATO 888) at different concentrations.

6.2.1.2.Optimization of surfactant

Single surfactants used in this study were poloxamer 188, lecithin, tween 20 and sodium deoxycholate and binary surfactants used were combination of poloxamer 188 with lecithin, tween and sodium deoxycholate, separately. Surfactants were chosen based on their different types and different physicochemical properties (Table 6.1). Selected surfactants vary with their molecular weight (MW) and HLB value. Thus, effects of different types of surfactants (including combinations of surfactants) and their effect on particle size, PDI, zeta potential, entrapment efficiency, surface morphology (scanning electron microscope and atomic force microscope) and stability upon storage were studied.

Table 6.1: Surfactants used and their properties

Surfactants	Poloxamer 188	Lecithin	Tween 20	Sodium deoxycholate
Type	Non-ionic	Zwitterionic	Non-ionic	Anionic
Molecular weight (daltons)	7680 – 9510	775	1230	400
HLB value	29	Variable (4, 7, 9)	16	16
Melting point	52-57**°C**	236**°C**	-	175°C

6.2.1.3.Optimization of processing parameters

In the present work, optimization of processing parameters for SLN preparation was done by using central composite design (CCD) and the data were analyzed using Design Expert® software (Trial version 9.0.3.1, Stat-Ease Inc., Minneapolis, MN, USA). The selected factors were homogenization speed (A), homogenization time (B), sonication time (C) and sonication intensity (D). Different ranges studied include homogenization speed of 5,000, 10,000 and 15,000 rpm, homogenization time of 15, 30 and 45 minutes, sonication time of 2.5, 5 and 7.5 minutes and sonication intensity of 40, 50 and 60 % amplitude. Optimization was performed to determine the optimal levels for less mean particle size (Y1), optimum PDI (Y2), and higher zeta potential (Y3). According to CCD, each factor was set to 5 levels: plus and minus alpha (axial points), plus and minus 1 (factorial points) and the centre point with α-value of 2 before generating the experimental design. The second-order polynomial equations were used to express the mean particle size, PDI and zeta potential of the SLN.

6.2.2. Characterization of SLN

6.2.2.1.**Particle size, PDI and zeta potential**

Particle size, PDI and zeta potential of SLN formulations were measured by using dynamic light scattering (Delsa^{TM} Nano C, Beckman coulter) technique. Samples were measured at a fixed angle of 165°at 25°C for particle size and PDI analyses. Average particle size, PDI, and zeta potential were measured in triplicate.

6.2.2.2.Surface morphology

Surface morphology of selected formulations was carried out by using scanning electron microscope (SEM 840 A, JEOL, Japan) and atomic force microscope (AFM) (NT-MDT Solver NEXT, Russia). For AFM analysis, few drops of aqueous nanosuspension were placed on small piece of clean microscope slide to form a film and the film was observed under AFM.

6.2.2.3.Entrapment efficiency

Entrapment efficiency (EE) of the optimized batch was determined by indirect method i.e. measuring the concentration of unentrapped drug in aqueous medium by centrifugation method and entrapped drug was determined from unentrapped drug concentration. Briefly, 1 ml of SLN formulations were taken in eppendroff tubes and centrifuged in a high speed cooling centrifuge (C-24, Remi) at 18,000 rpm for 45 min at 4°C. After centrifugation, supernatant was separated. The amount of unentrapped drug in supernatant was determined by using RP HPLC. Estimation was performed by determining the lupeol concentration in *Ficus religiosa* L. extract. RP HPLC (Waters, 5.5, USA) set up comprising of binary pump and PDA 2998 detector was used. Acetonitrile: methanol: water combination in the ratio of 40:40:20 was used as mobile phase. The mobile phase was filtered through 0.45 μm nylon filters (Millipore, USA). 20 μl volume samples were injected at the flow rate of 1 ml/min and analyzed at λ_{max} of 211 nm.

The percentage entrapment efficiency (% EE) was calculated by using the following formula:

$$\% \text{ EE} = \frac{\text{Total drug content-Unentrapped drug}}{\text{Total drug content}} \times 100$$

6.2.2.4.***In-vitro*** **release studies**

Dialysis bag diffusion method was used and two different diffusion mediums such as phosphate buffer, pH 6.8 and phosphate buffer, pH 7.4 were used. Dialysis membrane having molecular weight cut off 12,000 to 14,000 daltons was used for holding the samples. Before using, dialysis membrane was soaked in distilled water for 10 minutes and tied at one end. SLN dispersion equivalent to 50 mg of lupeol was filled in the dialysis membrane bag and tied at another end and this bag was placed in a beaker containing 100 ml of release medium. Temperature and speed were maintained at 37 ± 2°C and 100 rpm, respectively using magnetic stirrer. Samples were withdrawn at predetermined time intervals and withdrawn volume was replaced with same volume of buffer to maintain sink condition. Samples were analyzed at λ_{max} of 211 nm using RP HPLC. Cumulative percentage drug release was then calculated from the amount of drug released. The results of *in vitro* release studies were fitted into different kinetic equations such as zero order (cumulative % release vs. time), first order (log % drug remaining vs. time), and Higuchi's model (cumulative % drug release vs. square root of time). Values of r^2 and k were calculated for the linear curve obtained by regression analysis of the above plots. And for the Korse-Meyer–Peppas model, drug release values were fitted into log drug release vs. log time.

6.2.2.5.Stability studies

For selected samples, stability studies were carried out. For the surfactant effect study, samples that appeared to be stable by visual inspection (i.e. clear liquid, without phase separation, and any signs of solidification or gelation) were subjected to further analysis. Changes in particle size, PDI, zeta potential and entrapment efficiency were

measured. Results were expressed in standard deviation (SD). For the stability studies of best formulation after optimizing lipid, surfactant and processing parameters, samples were stored at 40° ± 2°C temperature and 75% ± 5% relative humidity for 180 days and were examined at regular time intervals for changes in particle size, PDI, zeta potential and % EE.

6.2.3. Preparation and characterization of optimized batch

From the optimization studies of lipid, surfactant and processing parameters, it was found that glyceryl monostearate as lipid at 2 % concentration, TPP, poloxamer 188 and sodium deoxycholate mixture in the ration of 25:75 was as surfactant, and 15,000 rpm homogenization speed for 30 minutes and 5 minutes sonication at 50 % amplitude to be optimum. With these optimized conditions, an optimized SLN batch was prepared by hot homogenization followed by ultrasonication method as mentioned in section 6.2.1. Then the optimized batch was characterized for particle size, PDI, zeta potential, surface morphology, *in vitro* release and kinetics and stability studies. SLNs with TPP were termed as targeted nanoparticles, without TPP, SLNs were termed as untargeted nanoparticles and SLNs with TPP and doesn't contain drug were termed as blank nanoparticles.

6.2.2.6.Fourier transform infrared studies

Standardized extract and lipid interaction was observed using FTIR-8400S, Shimadzu. FTIR spectrum of standardized extract, lipids used (glyceryl monostearate and compritol ATO 888) and their SLN formulations were obtained by conventional KBr disc/pellet method. The samples were prepared by grinding with anhydrous KBr powder and compressed into pellets. FTIR spectra were measured over the range of 4000 - 400 cm^{-1} with resolution of 4 cm^{-1} for 50 scans.

6.2.2.7.Differential scanning calorimetry

Thermograms of samples (standardized extract, lipids used (glyceryl monostearate and compritol ATO 888) and their SLN formulations) were obtained by using differential scanning calorimeter (DSC25, Toledo, Mettler). Samples were weighed directly in pierced DSC aluminium pan and scanned in the temperature range of 30 – 300°C under an atmosphere of dry nitrogen. Heating rate of 5°C/min was used and thermograms obtained were observed for interaction between extract and lipid.

6.2.2.8.Powder X-ray diffractometry

PXRD pattern of standardized extract, lipids used (glyceryl monostearate and compritol ATO 888) and their SLN formulations) were observed by using powder Xray diffractometer (X'Pert Pro PAN); Ni-filtered Cu-K radiation, voltage of 40 kV, and current of 1.5406 Å radiation scattered in the crystalline regions were used. Patterns were obtained by using a step size of 0.045°C with a detector resolution in 2θ (diffraction angle) between 5° and 80° at 25°C temperature.

6.2.3. Preparation and characterization of CdSe/ZnSe quantum dots

A separate formulation was prepared for studying the uptake of nanoparticles by mitochondria and thus, CsSe/ZnS quantum dots were incorporated into the optimized batch of SLN for imaging purpose. Cd/Se core QDs were prepared and characterized according to the reported method (Wankhede et al. 2008). Briefly, 0.587 g of cadmium acetate was dissolved in 25 ml of water by stirring, 85 ml of dimethyl formamide and 0.5 ml of mercaptoethanol were added, stirred for an hour and further 0.130 g of sodium sulphite was added. This was stirred for 15 minutes and refluxed for 90 minutes. Then, 0.025 g of selenium powder was added. After 3 hours of reflux, it was allowed to cool to room temperature. This solution is concentrated using rotary evaporator under vacuum. Acetone was added as an antisolvent which led to flocculation of particles. It was

centrifuged at 5,000 rpm for complete separation of solid. The resultant precipitate is dried and stored under vacuum till further analysis. Shelling of Cd/Se QDs by ZnS was carried out as per the reported method (Murcia et al. 2006). Briefly, zinc ethylxanthate (100 mg) was dissolved in 2 ml of tributylphosphine and added to CdSe core material which was placed in a reaction vessel. Then the solution was sonicated at 60 °C for 12 min until the reaction mixture reaches temperature of 120 °C.

Prepared quantum dots were characterized by UV-Visible spectroscopy, surface morphology, FTIR and PXRD. For estimating the absorption maxima, UV-Visible spectroscopy (FTIR-8400S, Shimadzu) was used. For surface morphology, SEM (JSM 5600, JEOL) was carried out by using a drop of sample, dried on a cover slip. IR spectroscopic measurements were carried out using FTIR-8400S, Shimadzu by conventional KBr disc/pellet method and measured over the range of 4000 - 500 cm^{-1} with resolution of 4 cm^{-1} for 50 scans. PXRD using X'Pert Pro PAN was used with the conditions of Ni-filtered Cu-K radiation, voltage of 40 kV, and current of 1.5406 Å radiations scattered in the crystalline regions. Patterns were obtained by using a step size of 0.045°Cwith a detector resolution in 2 θ (diffraction angle) between 5° and 80° at 25°C temperature.

6.2.4. Preparation and characterization of quantum dots incorporated SLNs

Firstly, SLNs were prepared by the combined method of hot homogenization and ultrasonication. Lipid was melted and *Ficus religiosa L.* extract, TPP and CdSe/ZnS QDs were dispersed in the melted lipid phase. Aqueous phase containing surfactant was poured into the lipid phase which was maintained at the same temperature of lipid phase. Lipid and its concentration, surfactant and its concentration and processing parameters were selected based on the optimization as mentioned under section 5.4. SLN suspension

was then allowed to cool to room temperature. Then, formed suspension was sonicated by using ultra-sonicator (200H, Hielscher). Prepared nanoparticles were characterized for particle size, PDI, zeta potential, entrapment efficiency, *in vitro* drug release and kinetics.

6.2.5. *In vitro* cytotoxicity assay

Cytotoxicity assessment of *Ficus religiosa L.* extract (at four different concentrations, 10 µg/ml, 25 µg/ml, 50 µg/ml and 100 µg /ml concentration), nontargeted nanoparticles and targeted nanoparticles and blank nanoparticles was performed by using MIN6 cell lines. Further, toxicity of TPP on nanoparticles surface was studied. Blank nanoparticles were prepared and different concentrations of TPP (0, 0.5 µmol, 1 µmol, 5 µmol and 10 µmol concentrations). MTT assay was performed on a 96-well plate, cells (1×10^5 cells/100 µl) were seeded into well plate. The cells were treated with *Ficus religiosa L.* extract, nontargeted nanoparticles, targeted nanoparticles and blank nanoparticles with different concentrations of TPP and incubated for 4 h at room temperature. After treating cells with 20 µl of MTT (5mg/ml in PBS) and incubated for 5 h. The plate was centrifuged for 5 minutes at 100×g at 4°C and the unreacted MTT was removed carefully by pipetting without disturbing the dark blue formazan (formed by cellular reduction of tetrazolium salt). To each well, 100µl of DMSO was added and then placed on a plate shaker for 5 min at room temperature to dissolve the crystals of formazan and the optical density was evaluated in an ELISA plate reader (Labsystem, Multiscan) at a wavelength of 540 nm. Percent cell viability was compared with untreated cells (control). Each experiment was performed in triplicate.

6.2.6. Mitochondrial uptake studies i*n vitro*

Isolated mitochondria were placed on glass slides and the dye, Rhodamine 123 was used for staining mitochondria. Formaldehyde (2%) and glutaraldehyde (2.5%) were

used for fixing the samples. Then the samples were observed under confocal microscope (LSM 510, Zeiss). Excitation and emission wavelength of 511 and 534 nm, respectively were used for rhodamine 123 and 543 and 574 nm for quantum dots.

6.2.7. *In vivo* studies

The study protocol used in the study was approved by the Central Animal Ethical Committee (Ref. No. Dean/2014/CAEC/718), Institute of Medical Sciences, Banaras Hindu University, Varanasi, India. Wistar rats of 220 ± 30 grams weight were used. All rats had free access to water and diet. They were housed in cages; a 12 h dark/light cycle was maintained throughout the study at room temperature (21–24 ° C), and relative humidity of 50% to 70%. General and environmental conditions were strictly monitored.

6.2.7.1.Induction of experimental diabetes

Diabetes was induced in rats by fructose fed and streptozotocin injection model. Fructose was given in drinking water of rats for over 24 days. Then single injection of streptozotocin was done intraperitoneally (streptozotocin, 40 mg/kg body weight was dissolved in 0.5 mL of citrate buffer, pH 4.5). After 7 days, the extent of diabetic induction was monitored based on blood–glucose level. Blood glucose levels were estimated using one touch glucometer. Blood glucose levels of at least 300 mg/dL were accepted as the basal level for diabetes.

6.2.7.2.Experimental design

The experimental design consists of five groups containing six rats each. Oral administration was performed. Group I (control) rats were administered with citrate buffer, group II (diabetic) rats were administered with citrate buffer, group III rats were administered with extract suspension (extract equivalent to 50 mg/kg body weight), group IV rats were administered with untargeted nanoparticles (extract equivalent to

50 mg/kg body weight) and group V rats were administered with targeted nanoparticles (extract equivalent to 50 mg/kg body weight). At the end of the experimental period, rats were subjected to euthanasia by anesthetizing with ketamine (50 mg/kg bodyweight, i.p.)

6.2.7.3.Isolation of mitochondria

Mitochondria from pancreas were isolated according to the reported method (Wilson et al. 1984). Immediately after sacrificing rats, pancreas was removed and placed in cold isolation medium (250 mM mannitol, 1 mM EDTA and 10 mM HEPES, pH 7.4) and homogenized. The homogenate was centrifuged at 750 g for 8 min at 4°C, and the supernatants were collected and centrifuged at 10,800 g for 10 min. The pellet was resuspended in the same medium without EDTA and centrifuged at 16,000 g for 5 minutes. The pellet was resuspended in the KCl-Trismedium, and then centrifuged again at 10,800 g for10 minutes. Obtained supernatant was further centrifuged at 750 g.

6.2.7.4.Assessment of mitochondrial morphology

Changes in mitochondrial morphology during oxidative stress of diabetes have been studied in diabetic group and nanoparticles treated group. Isolated mitochondria from pancreas were stained with Mitoview dye and were placed on glass slides. Fixation was done by using glutaraldehyde and paraformaldehyde in 0.1 M cacodylate buffer. Then the samples were observed under fluorescence microscope (Laica, Germany).

6.2.7.5.Complexes I, II, IV and V activity

The mitochondrial pellet was washed twice with 1 ml of homogenization buffer. The protein content of the pellet was assayed by the Bradford method. The mitochondrial pellet was subjected to “freeze-thawing” three times. Twenty microliters (0.3 mg of protein) of mitochondrial homogenate was mixed with 930 µl of 10 mM potassium phosphate buffer, pH 8.0, 50 µl of 100µM NADH. The rate of NADH oxidation was monitored at 350 nm for 2 min in a UV spectrophotometer. Then 5 µl of

10 mM ubiquinone-1 was added, and the stimulated rate of NADH oxidation was measured as complex I activity at 350 nm using extinction coefficient of 6.81 mM. Activity of NADH dehydrogenase was expressed as nanomole NADH oxidized per minute per milligram protein. Similarly, freeze thawed mitochondrial pellet was used for assessing the complex II, IV and V activities. Complex II (succinate dehydrogenase) was estimated by the reduction of nitroblue tetrazolium to diformazan at 570 nm and the activity was expressed in micromole formazan produced per minute per milligram of protein. Complex IV (cytochrome-c oxidase) was measured by the use of reduced form of cytochrome-c and the amount of oxidized form of cytochrome-c was measured at 550 nm and expressed in nanomole cytochrome-C oxidized per minute per milligram of protein. Complex V (ATP synthase) activity was assessed by the level of phosphate content in mitochondria suspended in ATPase buffer and the phosphate content was expressed in nanomole ATP hydrolysed per minute per milligram of protein.

6.2.7.6.Assessment of mitochondrial membrane potential

Mitochondrial membrane potential of isolated mitochondria was assessed by using fluorometric method (Spex Fluorolog-3 Spectrophotometer). Mitochondrial suspension was mixed with rhodamine 123 solution, incubated for 5 min at 25° C temperature. Unbound rhodamine 123 was removed by frequent washings. After suitable dilution with buffer, florescence emission was read at an excitation wavelength of λ 511 ± 10 nm and emission λ of 534 ± 10 nm using slit number 10. The results are expressed as fluorescence intensity value per milligram of protein (Palmeira et al. 2007).

6.2.7.7.Estimation of intracellular calcium ion concentration

Intracellular calcium ion concentration in isolated mitochondrial was estimated by standard titration method using Eriochrome black T as an indicator (Schatzmann and Vincenzi, 1969).

6.2.7.8.ROS levels estimation

ROS levels in the isolated mitochondria of control, diabetic and different treatment groups were estimated by the use of 2',7'-dichlorofluoresceindiacetate (DCFH-DA), fluorescence intensity produced by the conversion of DCFH-DA to a fluorescent compound 2',7'-dichloroflorescein (DCF). 100 µg of mitochondrial pellet was taken in a centrifuge tube containing mitochondrial suspending buffer, 50 µM of DCFH-DA was added to it and incubated for 30 minutes at 37°C for 30 min in dark. Then, washing was done by using PBS and the sample was transferred to a microscope slide and covered with a cover slip and the edges of the cover slip were sealed by using nail polish and viewed under fluorescence microscope (Laica, Germany) at excitation and emission wavelengths of 488 and 530 nm, respectively, and the mean fluorescence intensity of DCF was evaluated.

6.2.7.9.Estimation of antioxidants enzyme level

Superoxide dismutase was estimated according to the method of Kakkar *et al*. (Kakkar, Das et al. 1984). Briefly, 0.5 ml of mitochondria homogenate was diluted with distilled water followed by the addition of chilled mixture of ethanol and chloroform (2:1 ratio). This mixture was centrifuged at 4°C for 1 min. Supernatant was used for estimating enzyme activity. Assay mixture consisting of 1.2 ml of sodium pyrophosphate buffer (0.025 M, pH 8.3), 0.1 ml of 186 µM phenazolium methane sulphate, 0.3 ml of 30 µM nitro-blue tetrazolium chloride, 0.2 ml of 780 µM nicotinamide adenine dinucleotide was used for the assay. Homogenate was incubated with assay mixture for 30 min at 90° C and the reaction was stopped by adding 1 ml of glacial acetic acid. The reaction mixture was stirred vigorously and shaken with 4 ml of n-butanol. The intensity of the chromogen in the butanol layer was measured at λ_{max} of 560 nm against butanol blank. A system, free from enzyme, served as a control. One unit of enzyme activity is the enzyme

reaction which gave 50 % NBT reduction in one minute. The results were expressed as SOD activity/min/mg of protein (U/mg of protein).

Catalase activity was performed as per the method of Beers and Sizer (Beers and Sizer 1952). Mitochondrial homogenate was diluted to 10 times with PBS, pH 7.4. Diluted homogenate was mixed with 2 ml of H_2O_2 solution (in PBS). After 10 minutes, absorbance at 230 nm against a blank solution (PBS without H_2O_2) was measured. H_2O_2 concentration was determined using molar absorptivity of $81M^{-1}cm^{-1}$. Results were expressed as CAT activity/min/mg of protein (U/mg of protein).

Glutathione peroxidase activity was performed as per the reported method (Chu et al. 1993). 0.5 µg of mitochondria was taken in a microcentrifuge tube containing hydrogen peroxide and NADH in 0.1 M phosphate buffer. The conversion of NADPH to NADP was observed at 340 nm spectrophotometrically using molar absorptivity of 6.22 $M^{-1}cm^{-1}$ for NADH and the results were expressed as units per mg of protein.

6.2.7.10. Estimation of nitrite level and malondialdehyde formation

Protein present in the mitochondria was separated by the addition of 30 % $ZnSO_4$ and centrifuging the sedimented protein. Supernatant was incubated with metal cadmium for 12 hours which will cause the reduction of nitrate to nitrite. Amount of nitrite in sample was determined by using Griess reagent (Schulz, Kerber et al. 1999). Total nitric oxide level in terms of nitrite was measured at 550 nm spectrophotometrically and expressed as nmole/mg of protein.

For the determination of malondialdehyde formation, mitochondrial homogenate was added (1/10, v/v) to ice cold 1.15 % KCL solution and amalgamated with 0.1 ml of 8.1 % sodium dodecyl sulphate, 0.75 ml of 20 % acetic acid and 0.75 ml of 0.8 % thiobarbuturic acid (TBA). This mixture was diluted to 2.0 ml with distilled water and

heated at 95° C for 60 min. After cooling, 0.5 ml of distilled water and 2.5 ml of n-butanol/pyridine mixture (15:1, v/v) were added to the mixture and shaken vigorously. Later, mixture was centrifuged at 4,000 g for 10 minutes, (upper layer) was collected with a pipette. Absorbance of the collected organic layer was measured at λ_{max} of 532 nm. TBA reaction was standardized of 1,1,3,3-tetraethoxypropane standard solutions. Malondialdehyde concentration was expressed as nmole/mg of protein (Sunderman, Marzouk et al. 1985).

6.2.7.11. Western blotting of cytochrome-c, caspase-3 and -9

Protein (equivalent to 50 mg) present in the mitochondrial homogenate was precipitated by using trichloroacetic acid and the precipitated protein was fractionated by using 10 % SDS- PAGE and the bands of proteins were transferred to a polyvinylidene-difluoride membrane. Then, membranes were blocked for 2 hours in a buffer containing 5 % non-fat dry milk at room temperature. The membranes were then incubated with antibodies against cytochrome C (1:1,000 dilution), caspase-3 (1:1,000 dilution) and caspase-9 (1:1,000 dilution), separately.

6.2.7.12. Diabetes markers analysis

Blood glucose levels were measured by using one touch glucometer. . Insulin was estimated by using ELISA diagnostic kit (Nexus India) and followed as per manufacturer's instructions. Serum glycated haemoglobin was estimated as per the reported method (Nayak and Pattabiram 1981).

6.2.7.13. Histopathological studies

At the end of the study, all the animal groups were sacrificed by using anesthesia and different organs such as liver, pancreas, skeletal muscle, kidney and adipose tissue were isolated. Tissue isolated from different organs was fixed using formalin solution, dehydrated by alcohol and embedded in paraffin blocks. 5 µm sections were developed

using a semi-automated rotatory microtome, stained using hematoxylin and eosin and observed under light microscope.

6.2.7.14. Pharmacokinetic studies

For the pharmacokinetic assessment, twelve male Wistar rats weighing 220 ± 30 grams were used and they were divided into two groups containing six each (n=6). Group 1 and group 2 were administered with standardized extract suspension and optimized batch of SLN 2, respectively. Three more rats were used for calibrating lupeol in rat plasma.

6.2.7.14.1. Bioanalytical method development

For the estimation of lupeol in the *Ficus religiosa L.* standardized extract in rat plasma, RP HPLC method was developed. RP HPLC conditions were same as mentioned in the section 5.1.6.

6.2.7.14.2. Administration

The rats were fasted for 12 hours prior to dose administrations and for 4 hours after dosing. Extract suspension equivalent to 50 mg/kg of lupeol was administered orally into stomach of group 1 rats. SLN equivalent to 50 mg/kg of lupeol was administered orally into stomach of group 2 rats.

6.2.7.14.3. Plasma sample preparation

After drug administration, rats were anaesthetized with ether and heparinized capillary was inserted into retro-orbital vein of rats to collect 0.5 ml of blood at time intervals of 0.25, 0.5, 1.0, 2, 4, 8, 12, and 24 h. Blood samples were centrifuged at 5,000 rpm for 15 minutes and plasma samples were collected. It was stored immediately at −20°C until analysis. To 100 µL of plasma sample, 50 µL of methanol and 200 µL of acetonitrile were added to precipitate protein and vortexed (Remi, Cyclomixer, India) for

3 minutes. The denatured protein was separated by centrifugation at 15,000 rpm for 10 min at 4°C. Collected supernatant was transferred to fresh tube and filtered through 0.45 µm nylon filters. Aliquots of 20 µL were injected into the HPLC system for analysis.

6.2.7.14.4. Pharmacokinetic data analysis

To access the pharmacokinetic parameters (Cmax, Tmax, AUC, and $t_{1/2}$) of major compound present in *Ficus religiosa* L. extract, non-compartmental analysis was done by using WinNonlin software (Pharsight Corp., Mountain View, CA, USA, Version 4.1). *P*-value less than 0.05 was considered to be significantly different using paired student's t-test. All data were presented as mean ± SD.

6.3.Results and discussion

6.3.1. Optimization of lipid for the development of *Ficus religiosa* L. extract loaded SLN

For the preparation of SLN, several factors are to be considered which include effect of lipids, surfactants, processing parameters such as homogenization and sonication and formulation parameters (drug to lipid ratio) and stability. All factors are to be considered in the development phase of SLN as they have greater influence on size and charge of SLN, entrapment efficiency, stability during storage and drug release pattern. Optimization of SLN loaded with drug(s) is very important as each drug vary with their physiochemical properties which might have influence on size and charge of SLN. In this study, factors such as effect of lipids, surfactants and processing parameters were considered for the optimization of SLN.

Ficus religiosa L. extract loaded SLN were prepared by using hot homogenization followed by ultrasonication method. The followed method was found to be reliable, simple and reproducible. Prepared SLN formulations were found to be uniform and homogenous in appearance. To study the effect of lipids, two lipids were selected

(glyceryl monostearate and glyceryl behenate) and different concentrations of two lipids (1-5%) were studied. Ten formulations were prepared and the formulation codes assigned to them were SLN 1 – 10. The composition of ten formulations for the lipid effect study is given in the Table 6.2.

Table 6.2: Composition of SLN formulations

Ingredients	SLN 1	SLN 2	SLN 3	SLN 4	SLN 5	SLN 6	SLN 7	SLN 8	SLN 9	SLN 10
Drug (%)	0.5	0.5	0.5	0.5	0.5	0.5	0.5	0.5	0.5	0.5
GMS* (%)	0.5	1	2	3	4	-	-	-	-	-
GB# 888 (%)	-	-	-	-	-	0.5	1	2	3	4
Surfactant (%)	0.5	0.5	0.5	0.5	0.5	0.5	0.5	0.5	0.5	0.5
DW$ (ml)	50	50	50	50	50	50	50	50	50	50

*glyceryl monostearate, #glyceryl behenate$ distilled water, 0.5% concentration of poloxamer 188 was used as surfactant. Homogenization speed of 15,000 rpm and time of 30 minutes were used. Sonication was performed at 50% amplitude for 2 minutes.

6.3.1.1.Particle size, PDI and zeta potential

Results of particle size, PDI and zeta potential of all formulations are given in Table 6.3. It was observed that SLNs prepared by using glyceryl monostearate had particle size in the range of 154 to 195 nm and SLNs prepared by using compritol ATO 888 had particle size in the range of 202 to 287 nm. Increase in lipid concentration increased particle size which is independent of lipid type. Formulations

containing compritol ATO 888 (SLN 4 – 6) had higher particle size than formulations containing glyceryl monostearate (SLN 1 – 3). This increase in particle size of SLNs prepared by using compritol ATO 888 can be correlated with its higher melting point i.e. 72°C than GMS (59°C). Hence from the results, it was observed that higher the melting points of lipids, higher the particle size. Increase in lipid concentration (in both types) increased the PDI and had no effect on zeta potential.

Table 6.3: Size and charge analysis of all SLN batches

Formulations	Particle size (nm)	PDI	Zeta potential
SLN 1	154.0 ± 27.61	0.301 ± 0.03	48.47 ± 2.18
SLN 2	183.4 ± 30.64	0.312 ± 1.01	48.57 ± 5.64
SLN 3	195.4 ± 45.01	0.379 ± 0.74	49.76 ± 1.17
SLN 4	202.7 ± 33.47	0.457 ± 0.64	47.63 ± 3.48
SLN 5	256.3 ± 29.36	0.547 ± 0.90	43.21 ± 4.09
SLN 6	287.1 ± 41.89	0.599 ± 0.41	47.81 ± 3.68

Mean Values ± SD; n=3

6.3.1.2.Entrapment efficiency

From the results of EE, it was observed that increasing the lipid concentration increased the EE of both types of lipid (Table 6.4). Higher concentration of lipid is believed to provide more number of molecules to cover the drug molecules and also prevents drug leaching into external phase, thus, ensuring highest EE (Muller et al.,

2000). There was no significant change in EE of batches containing glyceryl monostearate and compritol ATO 888.

Table 6.4: Entrapment efficiency of all formulations

Formulations	Entrapment efficiency (%)
SLN 1	43.14 ± 1.34
SLN 2	56.13 ± 1.64
SLN 3	56.98 ± 2.11
SLN 4	43.65 ± 2.45
SLN 5	55.14 ± 1.97
SLN 6	56.17 ± 2.04

Mean ± SD; n=3

6.3.1.3.*In vitro* release studies

The release of lupeol from *Ficus religiosa* L. extract suspension was much faster with nearly 95% diffused into the release medium at 3rd hour in pH 1.2 for first two hours followed by H 6.8. SLN containing two different lipids displayed a similar biphasic drug release pattern with a burst release within 30 minutes followed by sustained release afterwards (Figure 6.1). The initial burst effect of the formulations containing glyceryl monostearate varied from 7.5% to 21.9 % (SLN 1–3); and for compritol 9.3–16.3% (SLN 4–6) and the burst release might be due to association of lupeol on the surface of nanoparticles. From the results, it was observed that higher the lipid ratio, higher the initial burst release. The sustained release of lupeol from the formulations containing

glyceryl monostearate were found to be 59.1%, 56% and 41.6% for SLN 1, 2 and 3, respectively; and compritol containing formulations (SLN 4, 5 and 6) showed 52.1%, 44.3%, and 28.1%, respectively, of drug release over 24 hours. The results revealed that the release was chiefly dependent on type and concentration of the lipids used i.e. increase in lipid concentration sustained the release rate which is independent of the lipids type. This might be due to increased viscosity of formulations by increase in lipid concentration which slows the drug release from the lipid matrix (Muller et al., 2000). Among the lipids used, compritol showed sustained release than glyceryl monostearate due to its longer carbon chain length. The release studies in pH 7.4 showed no significant difference in drug release (Figure 6.1B). All SLN formulations had higher linearity for Higuchi model.

From the combined results of *in vitro* characterization of all SLN batches, glyceryl monostearate at 2 % concentration was selected for further studies evaluations based on lesser particle size and higher entrapment efficiency.

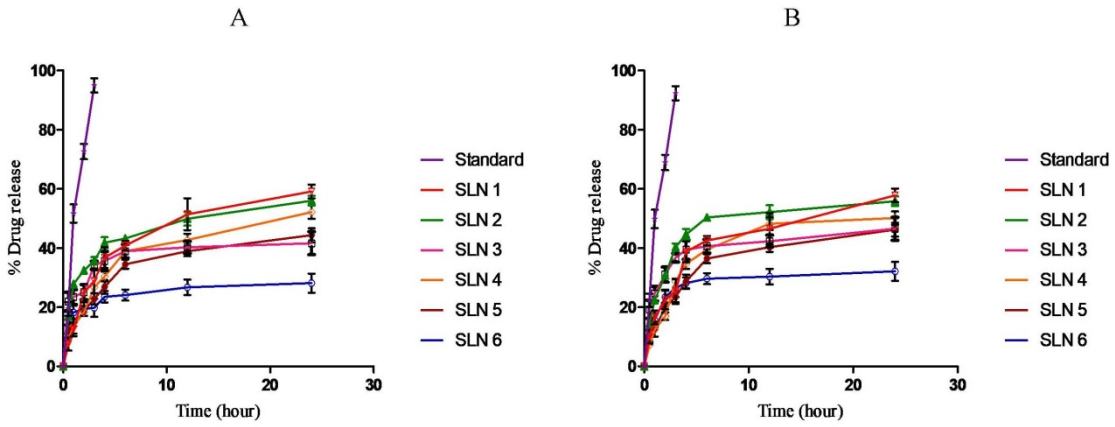

Figure 6.1. *In vitro* release profile of lupeol from standard and SLN formulations A) in pH 1.2 for first two hours followed by pH 6.8 and C)) in pH 7.4.

6.3.2. Optimization of surfactant

Surfactants used in SLNs act as stabilizer. Surfactants play vital role in preventing aggregation of particles by covering the surface of the nanoparticles thus maintaining the stability of particles. This happens by decreasing the surface tension between particles interface and thereby increasing the surface area of particles (Muller et al., 2000; Uner and Yener, 2007). Several types of surfactants are being used in the preparation of SLNs such as cationic surfactants (benzalkonium chloride, cetrimonium bromide), zwitterionic surfactants (lecithin), non-ionic surfactants (tween series, span series, poloxamer), anionic (sodium deodecylsulphate, dioctyl sodium sulfosuccinate) and amphoteric surfactants (imino propionates and imino acetates). Surfactants play a major role in deciding the particle size of particles i.e. when surfactant concentration is increased. Hence, we aimed to optimize surfactant which will give the most stable formulation along with lesser particle size and higher entrapment efficiency.

For the optimization of surfactant, 13 formulations were prepared by using single surfactants separately and by changing the ratios of binary surfactant combination. Composition of all SLN batches is given in Table 6.5.Glyceryl monostearate was used as lipid at 2 % concentration and processing parameters were set at 15,000 rpm as homogenization speed, 30 minutes as homogenization time, 50 % as sonication amplitude for 2 minutes.

6.3.2.1.Particle size and PDI

Particle size, PDI and zeta potential of all formulations are given in Table 6.6. Formulations prepared using single surfactants i.e. poloxamer 188, lecithin, tween 20 and sodium deoxycholate ($PO_{0.5,}$ $L_{0.5,}$ $T_{0.5,}$ and $SD_{0.5,}$ respectively) had particle size of 267.5 nm, 247.2, 264.4 nm and 315.0 nm, respectively. It was observed that lesser particle size was obtained with lecithin and higher particle size with

sodium deoxycholate. The order of surfactants with lesser particle size is lecithin> tween 20>poloxamer 188> sodium deoxycholate (Figure 6.2). Differences in particles size of formulations prepared using different surfactants can be correlated with their properties. Among the surfactants used, lecithin has molecular weight of 775 daltons resulted in lesser particle size, poloxamer 188 with molecular weight of 7680 daltons resulted in higher particle size and tween 20 of molecular weight, 1310 daltons existed in between. But in case of sodium deoxycholate (molecular weight of 400 daltons) had particle size of 315.1 nm which was higher than any of the surfactants used and which is irrespective of its molecular weight. Hence, increase in molecular weight of surfactant increases particles size. Similar to the molecular weight of surfactants, HLB value also had an impact on particle size i.e. lesser the HLB value, lesser the particle size which implied to all surfactants.

Table 6.5: Composition of all SLNs batches

S.No	Formulation code	Surfactant composition						
		PO	**L**	**T**	**SD**	**PO/L**	**PO/T**	**PO/SD**
Single surfactants								
1	$PO_{0.5}$	1	-	-	-	-	-	-
2	$L_{0.5}$	-	1	-	-	-	-	-
3	$T_{0.5}$	-	-	1	-	-	-	-
4	$SD_{0.5}$	-	-	-	1	-	-	-
Binary surfactants								
5	$PO_{25}L_{75}$	-	-	-	-	25:75	-	-
6	$PO_{50}L_{50}$	-	-	-	-	50:50	-	-
7	$PO_{75}L_{25}$	-	-	-	-	75:25	-	-
8	PO_{25} T_{75}	-	-	-	-	-	25:75	-
9	PO_{50} T_{50}	-	-	-	-	-	50:50	-
10	PO_{75} T_{25}	-	-	-	-	-	75:25	-
11	$PO_{25}SD_{75}$	-	-	-	-	-	-	25:75
12	$PO_{50}SD_{50}$	-	-	-	-	-	-	50:50
13	$PO_{75}SD_{25}$	-	-	-	-	-	-	75:25

PO-poloxamer, L – lecithin, T – Tween 20 and SD-sodium deoxycholate. Drug and lipid concentrations were kept constant as 100 mg and 2 %, respectively.

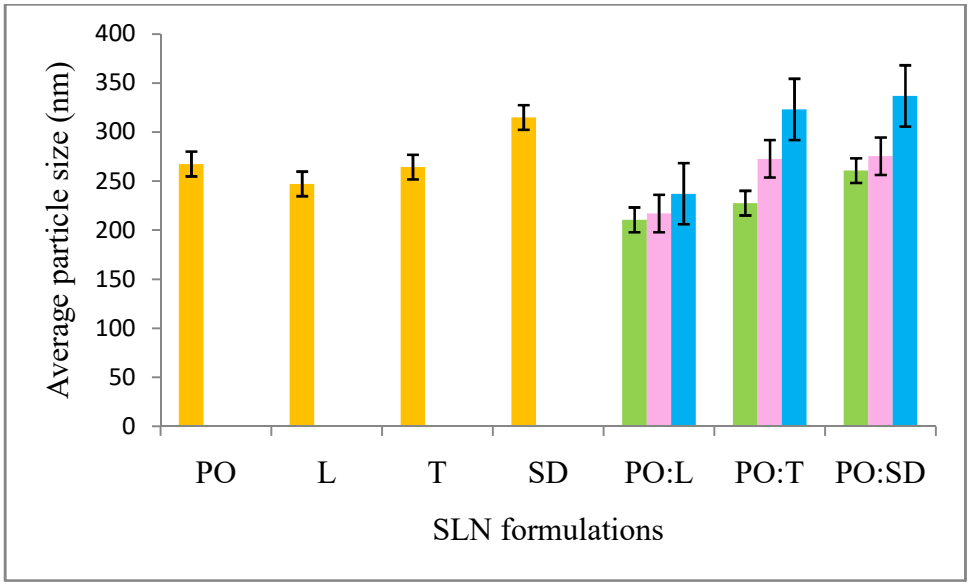

Figure 6.2. Average particle size of SLN formulations

PO – poloxamer 188, L – lecithin, T – tween 20, SD – sodium deoxycholate, PO:L – combination of poloxamer and lecithin in the ratio of 25:75 (green), 50:50 (pink), 75:25 (blue), PO:T – combination of poloxamer and tween 20 in the ratio of 25:75, 50:50, 75:25, and PO:SD – combination of poloxamer and sodium deoxycholate in the ratio of 25:75, 50:50, 75:25.

Table 6.6: Particle size, PDI and zeta potential of all formulations

S. No.	Formulation code	Particle size (nm)	PDI	Zeta potential (mV)
Single surfactants				
1	$PO_{0.5}$	267.5	0.493	39.04
2	$L_{0.5}$	247.2	0.374	-35.33
3	$T_{0.5}$	264.4	-0.655	39.04
4	$SD_{0.5}$	315.0	-0.433	**-52.70**
Binary surfactants				
5	$PO_{25}L_{75}$	**210.6**	0.453	-28.72
6	$PO_{50}L_{50}$	217.0	0.610	-30.67
7	$PO_{75}L_{25}$	237.2	0.451	-35.98
8	PO_{25} T_{75}	227.6	0.565	36.74
9	PO_{50} T_{50}	272.8	0.313	46.70
10	PO_{75} T_{25}	323.2	0.324	43.80
11	$PO_{25}SD_{75}$	261.8	**0.312**	-41.66
12	$PO_{50}SD_{50}$	269.5	0.471	-42.86
13	$PO_{75}SD_{25}$	283.9	0.340	-42.54

In case of formulations with binary surfactants, increase in concentration of primary surfactant (poloxamer 188) concentration and decrease in secondary surfactant (lecithin, tween 20 and sodium deoxycholate) concentration i.e. 25:75, 50:50 and 75:25 (poloxamer 188 as primary surfactant and others being secondary surfactants) resulted in increased particle size which was independent of the surfactant type. Among the different surfactant combinations (poloxamer:lecithin; poloxamer:tween 20 and poloxamer:sodiumdeoxycholate) used, poloxamer:lecithin had lesser particle size and poloxamer:sodiumdeoxycholate had higher particle size which was near to poloxamer:tween 20 combination. The order of surfactant combinations with lesser particle size is poloxamer:sodiumdeoxycholate < poloxamer:tween 20 < poloxamer:lecithin. This may be due to the reason that when primary surfactant concentration was increased, it resulted in higher concentration but number of molecules required for stabilization decreased as it has higher molecular weight. And when the secondary surfactant concentrations were increased, it resulted in higher number of molecules for stabilization thereby, reducing the particle size.

In PDI analysis, PDI values ranging between 0.374 and 0.655 were obtained with formulations containing single surfactants. In case of formulations containing binary surfactants, PDI values were between 0.312 and 0.610. Narrow particle size distribution was obtained with formulations containing binary surfactants than single surfactants. Increase in primary surfactant concentration from 25:75 to 50:50 increased PDI value and further increase to 75:25 decreased PDI in all types of surfactant. In formulations with binary surfactants, poloxamer : sodium deoxycholate had lower PDI value than poloxamer:lecithin and poloxamer : tween 20 combinations. This may be due to lower molecular weight of sodium deoxycholate than other surfactants.

6.3.2.2.Zeta potential:

In general, zeta potential gives information about stability of nanoparticles. Higher the zeta potential values, higher the stability. Interestingly, from the results, it was found that zeta potential values of SLNs formulations with single surfactants were more than those of formulations with binary surfactants. Among all single surfactants used, sodium deoxycholate had higher zeta potential value (-52.70). In formulations with binary surfactants, zeta potential values ranged between 28.72 and 46.70. Increase in primary surfactant concentration had an impact on zeta potential values i.e. zeta potential value increased first and then decreased. Also, surfactant with low HLB, e.g. lecithin of 4 HLB value had lesser zeta potential than surfactants with high HLB values (tween 20 and sodium deoxycholate of 16).

6.3.2.3.Entrapment efficiency

The entrapment efficiency (EE) values of all formulations are given in Table 6.7. It was observed that formulations with binary surfactants had higher entrapment efficiency than formulations with single surfactant. Among the single surfactants used, sodium deoxycholate showed lesser EE and poloxamer 188 showed higher EE and tween 20 and lecithin exhibited in between. This can be correlated with the molecular weight of the single surfactants used. Of the surfactants used, sodium deoxycholate has lesser molecular weight and poloxamer 188 of higher molecular weight and lecithin and tween 20 existed in between. Hence, higher the molecular weight of surfactants used, higher the entrapment efficiency. These results are in consistent with particle size analysis except for sodium deoxycholate.

In case of binary surfactant combinations, increase in concentration of poloxamer 188 in binary surfactants increased entrapment efficiency which could be due to its higher alkyl chain that helps in accommodating more entrapped drug. Of the combinations used

(PO:L, PO:T and PO:SD), PO:L showed higher entrapment efficiency but the formulation was more viscous in nature. There was no much difference in EE of PO:T and PO:SD but PO:SD was found to be clear suspension.

Table 6.7: Entrapment efficiency of all formulations

S.No	Formulation code	% Entrapment efficiency
1	$PO_{0.5}$	34.65 ± 0.75
2	$L_{0.5}$	28.51 ± 2.35
3	$T_{0.5}$	29.65 ± 1.57
4	$SD_{0.5}$	22.78 ± 0.99
5	$PO_{25}L_{75}$	60.24 ± 1.24
6	$PO_{50}L_{50}$	66.58 ± 0.74
7	$PO_{75}L_{25}$	68.75 ± 0.56
8	PO_{25} T_{75}	54.87 ± 1.81
9	PO_{50} T_{50}	59.68 ± 1.77
10	PO_{75} T_{25}	62.35 ± 0.36
11	$PO_{25}SD_{75}$	55.47 ± 1.40
12	$PO_{50}SD_{50}$	60.45 ± 3.21
13	$PO_{75}SD_{25}$	64.58 ± 2.12

Mean ± SD (n=3)

6.3.2.4.Surface morphology

SEM images of formulations with both single surfactants and binary surfactants are shown in Figure 6.3. SEM study revealed the actual morphology of SLNs. Particle size of SLNs observed by SEM was well correlated with size measurement done by using DelsaNano^{TM} C. From the SEM image of SLNs, it was observed that all the particles were in nano size range and in spherical shape. Interestingly, it was observed that SLNs

were more colloidal or viscous in nature in case of formulations with single surfactant and clear spherical particles were observed in formulations with binary surfactants.

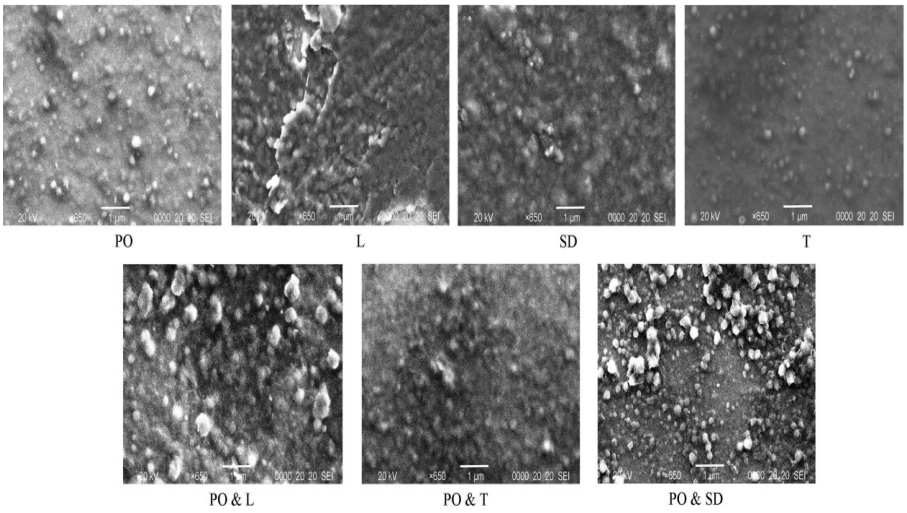

Figure 6.3. SEM images of SLN formulations prepared using single and binary surfactants

6.3.2.5.**Stability studies:**

Results of stability studies of all SLNs formulations are given in Table 6.8. It was observed that formulations containing poloxamer (as single surfactant), lecithin (both as single and binary combinations) became very viscous after 180 days of storage which were very difficult to re-disperse and thus increase in particle size. This could be due to increased molecular weight of poloxamer 188 and increased viscosity of both poloxamer 188 and lecithin. Tween 20 containing formulations have increased viscous nature but were easy to redisperse with increase in particle size than sodium deoxycholate but lesser than poloxamer 188 or lecithin. This might be because of tween 20's low critical micelle

concentration (0.06 mM) and hence surfactant monomer concentration in continuous phase will be relatively low. Further, as it is surfactant monomers (rather than micelles) that adsorb to hydrophobic surfaces, it would not be to fully stabilize SLNs against particle aggregation, even at higher concentrations. In case of formulations containing sodium deoxycholate (both as single and binary combinations), they retained suspension nature of SLNs and hence, very easy to redisperse.

During storage period, there were significant changes in particle size of SLNs formulations prepared with single surfactants (Table 6.9). But in case of SLNs formulations prepared with binary surfactants, there were fewer changes in particle size which was found to be less than formulations containing single surfactants. In formulations prepared with single surfactants, particle size ranged between 1062 nm and 3040 nm at 180 days of storage. Of all single surfactants used, sodium deoxycholate had lesser particle size (1062 nm) but was in micron range after 6 months of storage. Hence, it was observed that none of the single surfactants have the ability to retain particle size minimum. In formulations with binary surfactants, particle size ranged from 349 to 1530 nm at 180 days of storage. Among the three binary surfactants combinations used, poloxamer 188: sodium deoxycholate combination had lesser particle at 0 day and rate of particles aggregation happened slowly after 180 days of storage.

From the results, we are assuming the theory that in case of formulations containing single surfactants, particles are covered with single surfactant layer. Upon storage, disruption of surfactant layer occurs which results in decreased particles aggregation prevention. Further storage results in further disruption of surfactant layer and eventually results in aggregation of particles as shown in Figure 6.4. In case of formulations containing binary surfactants, particles are covered with two surfactant

layers, first coating being the first surfactant layer and second coating being second surfactant layer. Upon storage, disruption of first surfactant layer occurs but not in second surfactant layer. Further storage results in further disruption of first surfactant layer and very less disruption in second surfactant coating. This leads to very less particles aggregation. From the results, it is concluded that lesser particle size was observed particularly in case of binary combination and higher particle size was observed in single surfactants and binary surfactant combinations found to be effective in surface aggregation prevention of SLNs. Also, results revealed that poloxamer 188: sodium deoxycholate binary mixture combination was suitable for stabilizing SLNs formulations in the ratio of 25:75. There were no significant differences in PDI and zeta potential of formulations containing binary surfactants

Table 6.8: Stability studies of all formulations after 180 days of storage

S.No.	Formulation code	Phase separation	Solidification or gelation	Redispersibility
1	$PO_{0.5}$	---	++	++
2	$L_{0.5}$	---	---	+++
3	$T_{0.5}$	---	---	+++
4	$SD_{0.5}$	---	---	+++
5	$PO_{25}L_{75}$	---	---	+++
6	$PO_{50}L_{50}$	---	--	++
7	$PO_{75}L_{25}$	---	+	---
8	PO_{25} T_{75}	---	---	+++
9	PO_{50} T_{50}	---	++	++
10	PO_{75} T_{25}	---	+++	---
11	$PO_{25}SD_{75}$	---	---	+++
12	$PO_{50}SD_{50}$	---	---	++
13	$PO_{75}SD_{25}$	---	---	---

(+) symbol indicates positive response and the ratings are (+) - slightly, (++) - normal (+++) - very severe, (-) symbol indicates no response and the rating (-) - slightly, (--) - normal (---) - very severe

Table 6.9: Particle size, PDI and zeta potential of all formulations during 180 days of storage

Formulation code	0 day			180 days		
	PS	PDI	ZP	PS	PDI	ZP
$PO_{0.5}$	267.5	0.493	39.04	2857.4	0.490	32.71
$L_{0.5}$	247.2	0.374	-35.33	2890.1	0.508	-37.38
$T_{0.5}$	264.4	0.433	39.04	3040.6	2.153	41.30
$SD_{0.5}$	315.0	0.655	-52.70	1062.0	0.179	-40.61
$PO_{25}L_{75}$	210.6	0.453	-28.72	1530.1	0.387	-25.52
PO_{25} T_{75}	227.6	0.565	36.74	963.1	0.504	27.47
$PO_{25}SD_{75}$	261.8	0.112	-42.86	349.0	0.167	-38.56

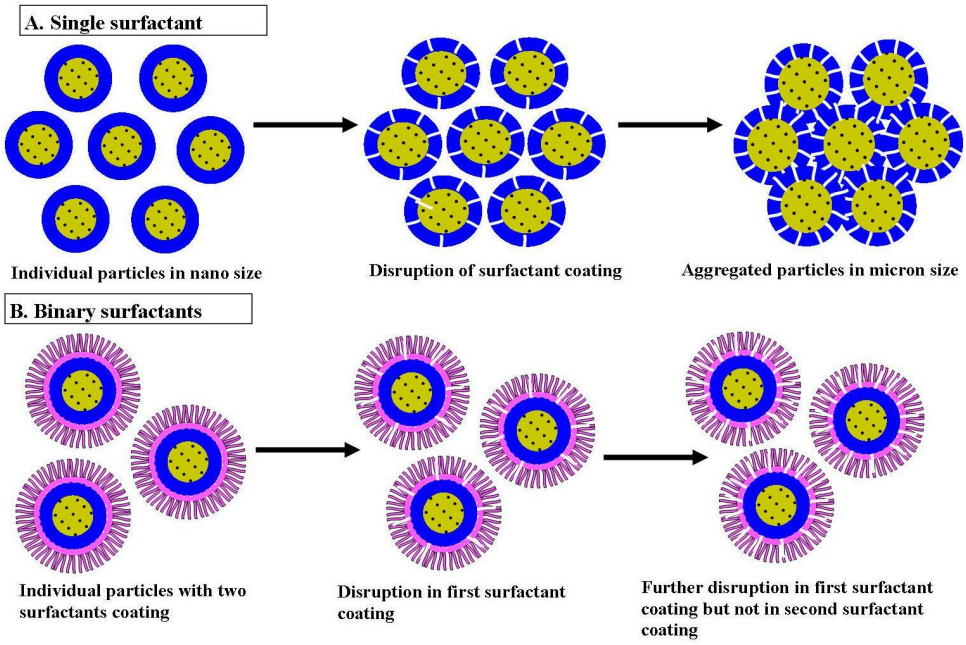

Figure 6.4.Diagrammatic representation of mechanisms of increase in particle size of SLNs prepared using single surfactants and maintenance of particle size of SLNs with binary surfactants

None of the formulations with single surfactants retained EE during storage for 180 days. Of the surfactants used poloxamer 188 had higher EE after 180 days but it had a vast difference of EE from day 0. This could be due to disruption of single surfactant coating during storage and this led to more drug leaching from the solid lipid matrix (Figure 6.5). But in case of formulations with binary surfactants, all of binary combinations maintained EE after 180 days of storage as shown in Table 6.10. This might be due to combined effect of poloxamer 188 with other secondary surfactants used (lecithin, tween 20 and sodium deoxycholate). Also, binary surfactants form two surface coatings. The time required to break these surface coatings is higher than single surface coating in case of single surfactant. These two effects prevented or sustained the drug leaching from solid matrix to aqueous phase. In case of single surfactants, EE was comparatively low than those of binary surfactants but in case binary surfactants after 180 days of storage, all of the three binary combinations used had similar EE. This might be due to incorporation of poloxamer 188 in all the three combinations which improved the EE.

From the effect of single and binary surfactants on stability of SLNs formulations, interesting results were obtained. Formulations with single surfactants showed higher particle size and PDI than formulations with binary surfactants and had lesser entrapment efficiency than binary surfactants. Formulations with single surfactants failed to maintain the stability during 180 days of storage whereas formulations with binary surfactants maintained stability. Of the binary surfactants combinations studied, poloxamer 188 with sodium deoxycholate maintained higher stability compared to binary combinations of poloxamer 188 with lecithin or tween. Hence, combination of poloxamer 188 and sodium deoxycholate in the ration of 25:75 was selected for further evaluations.

Table 6.10: Entrapment efficiency of all formulations during after 180 days of storage

S. No.	Formulation code	% Entrapment efficiency	
		0 day	180 days
Single surfactants			
1	$PO_{0.5}$	34.65 ± 0.75	22.14 ± 1.64
2	$L_{0.5}$	28.51 ± 2.35	12.33 ± 0.58
3	$T_{0.5}$	29.65 ± 1.57	11.75 ± 0.32
4	$SD_{0.5}$	22.78 ± 0.99	9.38 ± 1.36
Binary surfactants			
5	$PO_{25}L_{75}$	60.24 ± 1.24	59.58 ± 0.77
6	$PO_{50}L_{50}$	66.58 ± 0.74	63.87 ± 0.56
7	$PO_{75}L_{25}$	68.75 ± 0.56	65.40 ± 0.11
8	PO_{25} T_{75}	54.87 ± 1.81	53.46 ± 0.95
9	PO_{50} T_{50}	59.68 ± 0.18	58.23 ± 0.30
10	PO_{75} T_{25}	62.35 ± 0.36	59.91 ± 2.45
11	$PO_{25}SD_{75}$	55.47 ± 1.40	53.54 ± 1.68
12	$PO_{50}SD_{50}$	60.45 ± 3.21	57.68 ± 1.11
13	$PO_{75}SD_{25}$	64.58 ± 2.12	61.69 ± 0.52

Mean ± SD (n=3)

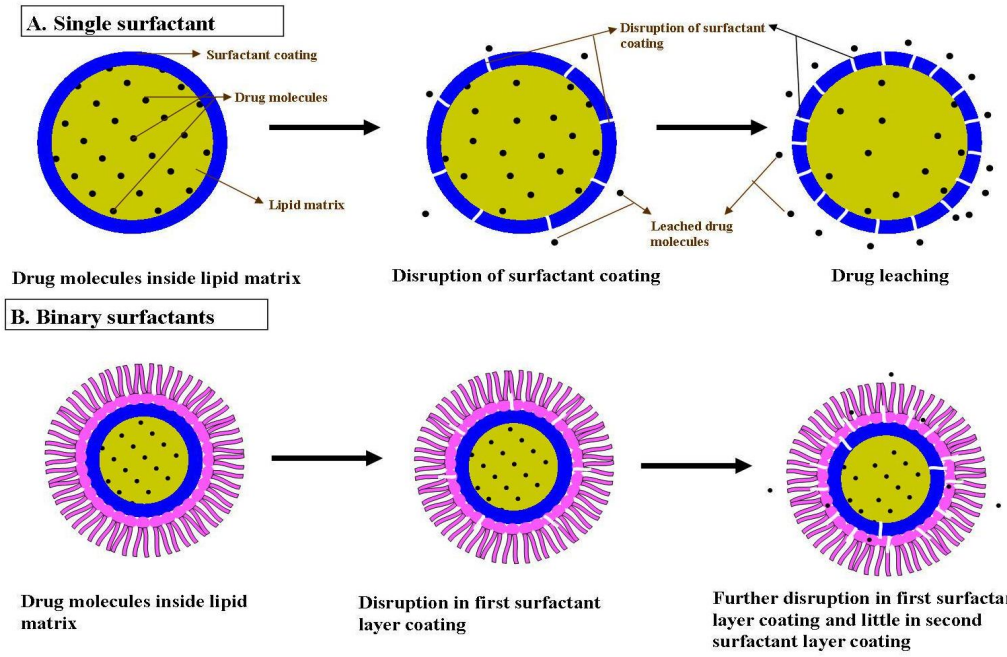

Figure 6.5. Diagrammatic representation of mechanisms of drug leaching from SLNs prepared using single surfactant and binary surfactants

6.3.3. Optimization of processing parameters

Processing parameters have greater influence on particle size, PDI and zeta potential which eventually affect the stability of the particles during storage. In case of processing parameters effect, two techniques are widely used to disperse the particles. They are high shear homogenization and ultrasonication. Homogenization is the process of converting two immiscible liquids into emulsion. High shear/pressure homogenizers push a liquid with high pressure through a narrow gap and thus, the fluid accelerates on a very short distance to very high velocity (Muller et al. 2000). This high shear stress and cavitation forces disrupt the particles resulting in particle size reduction (Mehnert et al. 2001). Ultrasonication is the process of applying sound energy (>20 kHz) to agitate particles in a sample (Jamei et al. 2014). Both homogenization and ultrasonication have greater effect on size and charge of particles. Hence, it is necessary to optimize these two parameters to obtain SLN with lesser particle size, optimum PDI and higher zeta potential.

For optimization, the effect of different variables on nanoparticles should be considered and optimization is done by changing single variable and keeping other variables as constants. This is time consuming process and also it does not allow studying the combined effect of variables. A factorial design approach or response surface methodology (RSM) is applied to minimize number of experiments and to study the combined effect of variables/factors together which is time effective. RSM is a collection of statistical and mathematical techniques useful for developing, improving and optimizing processes. It is widely used in the design, development and formulation of new products/formulations and improvement of existing product design (Bas et al. 2007).

Optimization of processing parameters was done by using central composite design (CCD) and the data were analyzed using Design Expert® software (Trial version 9.0.3.1,

Stat-Ease Inc., Minneapolis, MN, USA). The selected factors were homogenization speed (A), homogenization time (B), sonication time (C) and sonication intensity (D). Different ranges studied include homogenization speed of 5,000, 10,000 and 15,000 rpm, homogenization time of 15, 30 and 45 minutes, sonication time of 2.5, 5 and 7.5 minutes and sonication intensity of 40, 50 and 60 % amplitude. Optimization was performed to determine the optimal levels for less mean particle size (Y1), optimum PDI (Y2), and higher zeta potential (Y3). According to CCD, each factor was set to 5 levels; plus and minus alpha (axial points), plus and minus 1 (factorial points) and the centre point with α-value of 2 before generating the experimental design. The software had generated a total of 30 runs (Table 6.11). The second-order polynomial equations were used to express the mean particle size, PDI and zeta potential of the SLNs.

Table 6.11: Experimental design generated by central composite design

Run	A:Homogenization speed (rpm)	B:Homogenization time (min)	C:Sonication time(min)	D:Sonication intensity (% Amp)
1	20000	30	5	50
2	10000	30	5	50
3	15000	15	2.5	40
4	10000	30	10	50
5	15000	45	7.5	40
6	15000	15	7.5	40
7	10000	60	5	50
8	10000	30	5	30
9	15000	45	2.5	60
10	10000	30	5	70
11	5000	15	2.5	40
12	15000	15	2.5	60
13	5000	30	5	50
14	5000	45	2.5	40
15	5000	15	7.5	40
16	10000	30	5	50
17	10000	30	2.5	50
18	15000	30	5	50
19	15000	45	7.5	60
20	5000	15	7.5	60
21	5000	45	7.5	40
22	5000	15	2.5	60
23	15000	30	5	40
24	10000	15	5	50
25	5000	45	2.5	60
26	15000	30	5	50
27	15000	45	2.5	40
28	5000	45	7.5	60
29	10000	45	5	50
30	15000	15	7.5	60

6.3.3.1.Statistical analysis

Optimization of *Ficus religiosa L.* extract loaded SLN was carried out by CCD using Design Expert software. Four factors include homogenization time, homogenization speed, sonication time and sonication intensity and three responses include particle size, PDI and zeta potential were studied. The experimental data were used to calculate the regression coefficients of the quadratic polynomial equations and the significance of

each regression coefficient was statistically evaluated by Analysis of Variance (ANOVA).

Variance inflation factors (VIF) quantifies the severity of multi-collinearity in an ordinary least squares regression analysis. It provides an index of increased variance because of collinearity. Ideal VIF value is 1.0. In the least squares regression analyses of the tested four factors, VIF values were ranging between 1.0 and 1.18. *R-squared* value is a *statistical* measure of how closely the data are fitted on the regression line. Ideal R-squared value is 0.0. From the tested data, R-squared values were ranging between 0 and 0.2004. Other statistical analysis of the experimental design by CCD is given in Table 6.12. Co-efficient values and p-values of particle size, PDI and zeta potential from the experimental design are given in Table 6.13. From the statistical analysis of the experimental design by CCD, it was found that the experimental design had accuracy with ideal values of VIF and R-squared.

Table 6.12: Statistical analysis of the experimental design

Statistical analysis	Particle size	PDI	Zeta potential
Std. Dev.	269.33	0.11	3.63
Mean	796.10	0.49	35.58
C.V. %	33.83	21.66	10.20
Press	3.386E+006	0.92	881.93
R-Squared	0.8907	0.7111	0.9413
Adjusted R-Squared	0.8135	0.4415	0.8865
Predicted R-Squared	0.6999	-0.5872	0.7378
Adeq. Precision	11.879	6.230	15.702

Table 6.13: Co-efficient values and p-values of responses from the experimental design

Model	Particle size		PDI		Zeta potential	
	Co-efficient	p-value	Co-efficient	p-value	Co-efficient	p-value
	18.94	< 0.0001	2.64	0.0362	17.18	< 0.0001
A	193.83	< 0.0001	29.74	<0.001	200.21	< 0.0001
B	18.85	0.0006	1.03	0.214	0.10	0.7536
C	14.98	0.0015	1.68	0.3144	8.05	0.0125
D	0.83	0.3766	0.013	0.9122	1.11	0.3082
AB	1.23	0.2840	1.74	0.2072	0.81	0.3817
AC	0.49	0.4938	0.46	0.2072	0.45	0.5110
AD	1.57	0.2301	0.058	0.8122	6.06	0.0265
BC	0.25	0.6274	0.097	0.7594	0.40	0.5357
BD	0.49	0.4935	0.094	0.7630	0.088	0.7711
CD	1.556	0.9691	1.337	0.9772	1.19	0.2925
A^2	0.42	0.5246	0.083	0.7772	0.54	0.4753
B^2	2.96	0.1061	0.074	0.7887	0.19	0.6730
C^2	6.82	0.0197	0.36	0.4133	3.79	0.0704
D^2	0.11	0.7400	0.26	0.9761	0.16	0.6973

6.3.3.2.Effects on particle size

According to the regression coefficients calculated for the particle size response (Y1), the model can be represented by the following equation:

$Y1 = 656.503 - 504.471 * A - 230.862 * B - 186.138 * C + 8.11063 * D + 190.356 * AB + 40.9186 * AC + 29.1922 * AD + 40.9313 * BC + 8.84375 * BD - 0.457312 * CD + 87.8267 * A^2 + 62.306 * B^2 + 146.062 * C^2 - 40.2814 * D^2$

The coefficients of determination (R^2) and adjusted R^2 for Y1 were found to be 0.7111 and 0.4415, respectively, and the lack of fit was considered to be marginally non-significant (p = 0.010) indicating that the model appropriately explains the variability of the observed responses. Mean particle size varied from 180 nm to 2087 nm. Increase in homogenization time and homogenization speed decreased particle size. The three-dimensional response surface plots for particle size are

presented in Figure 6.6A. Increase in homogenization speed from 5,000 rpm to 15,000 rpm tremendously decreased the mean particle size of SLN. Further increase in homogenization speed to 20, 000 rpm did not result in significant reduction of particle size. Similarly, in case of homogenization time, increase in homogenization time (from 15 minutes to 30 minutes) decreased the particle size of SLN and further increase had no effect. Different sonication times of 2.5, 5 and 7.5 minutes have been studied. Increase in sonication time from 2.5 to 5 minutes decreased particle size effectively and further increase in sonication time to 7.5 minutes had no effect on particle size reduction. Sonication intensity had no effect on particle size (Figure 6.6B).

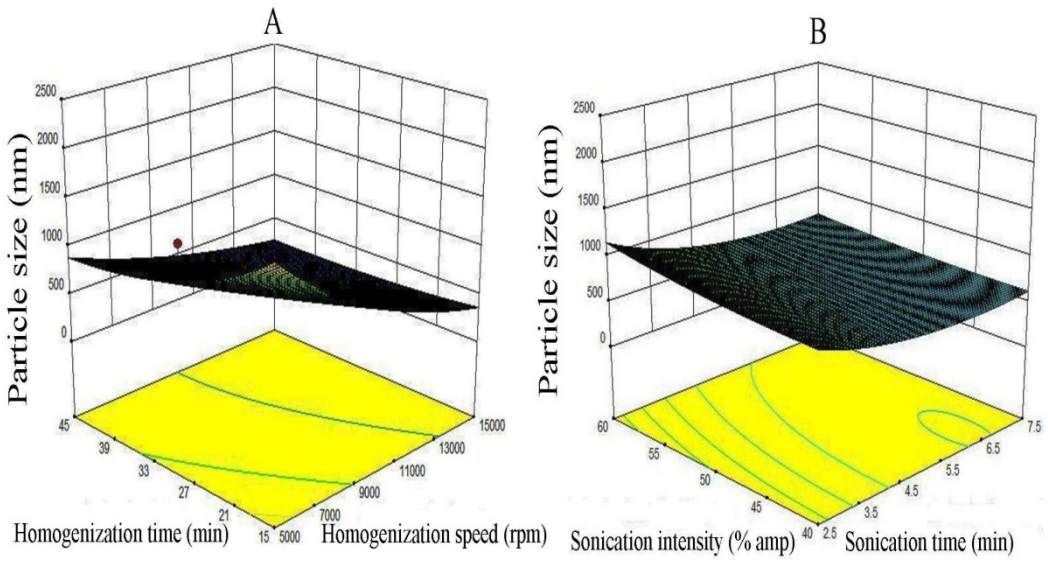

Figure 6.6. 3D images of A - effect of homogenization speed and time on particle size and B - effect of sonication time and intensity on particle size

6.3.3.3.Effects on PDI

PDI is a measure of distribution of sizes of particles. Lesser the PDI value narrower the particle size distribution. In general, PDI less than 0.5 is considered as optimum for

nanoparticles and PDI more than 0.5 shows polydisperse system and if it is closer to zero it denotes the monodisperse system. Polydisperse have greater tendency to aggregate than monodisperse system. PDI value of all SLN formulations ranged from 0.314 to 0.863. According to the regression coefficients calculated for the PDI response (Y2), the model can be represented by the following equation:

$Y2 = 0.512111 - 0.113197 * A - 0.0243693 * B - 0.0273004 * C - 0.00244921 * D + 0.034875 * AB + 0.0174037 * AC + 0.00623315 * AD - 0.00825 * BC + 0.008125 * BD + 0.000291469 * CD - 0.00644951 * A^2 - 0.00763736 * B^2 + 0.0129732 * C^2 - 0.0109501 * D^2$.

The R^2 and adjusted R^2 for Y2 were found to be 0.9413 and 0.8865, respectively, and the lack of fit was considered to be marginally non-significant ($p = 0.010$) indicating that model appropriately explains the variability of the observed responses. All the four factors (homogenization time, homogenization speed, sonication time and sonication intensity) had positive effect on PDI (Figure 6.7 A and B). PDI value of 0.314 was obtained at homogenization speed of 15,000 rpm, homogenization time of 30 minutes, sonication time of 5 minutes and sonication intensity of 50 % amplitude. These optimized conditions were same as for obtaining lesser particle size. Increase in PDI values up to 0.8 were obtained with lesser homogenization speed, homogenization time, sonication time and sonication intensity.

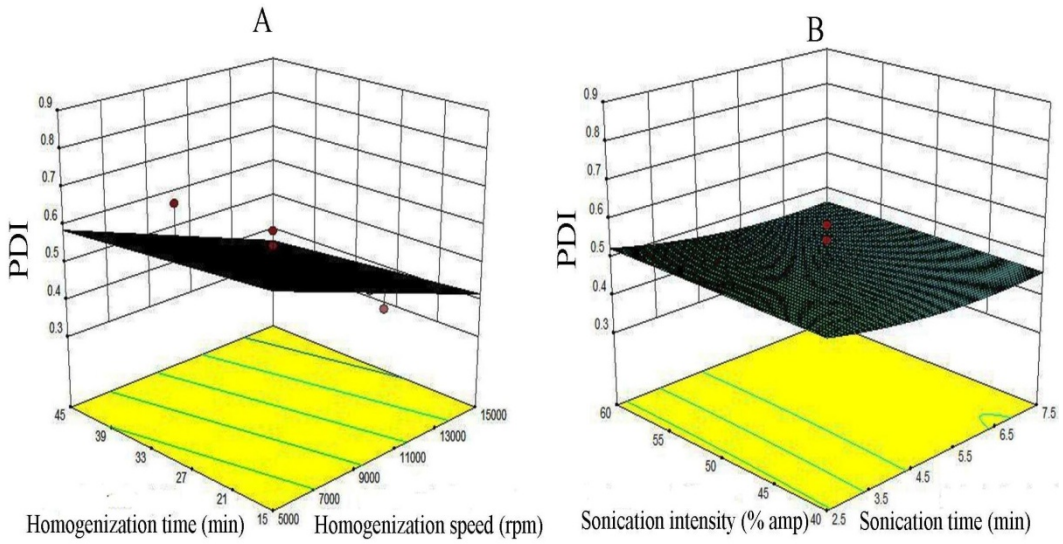

Figure 6.7. 3D images of A - effect of homogenization speed and time on PDI and B - effect of sonication time and intensity on PDI

6.3.3.4.Effects on zeta potential

Zeta potential can be described as the electric potential difference across the ionic layer around a charged ion in colloids. Higher the zeta potential value, lesser the particles aggregation. According to the regression coefficients calculated for the zeta potential response (Y3), the model can be represented by the following equation:

$Y3 = 34.9565 + 10.0713 * A - 0.263579 * B + 2.04811 * C - 0.790154 * D + 0.8175 * AB + 0.59517 * AC - 2.17552 * AD - 0.575 * BC + 0.26875 * BD + 0.942736 * CD + 0.562105 * A^2 + 0.413215 * B^2 - 1.44591 * C^2 - 0.293941 * D^2$

The R^2 and adjusted R^2 for Y3 were found to be 0.8135 and 0.6999, respectively, and the lack of fit was considered to be marginally non-significant ($p = 0.031$) indicating that the model appropriately explains the variability of the observed responses. In all the SLN batches, zeta potential value ranged from 21 mV (lowest) and 57.31 mV (highest). Homogenization time and homogenization

speed had greater effect on zeta potential whereas sonication time and sonication intensity had little effect on zeta potential. The three-dimensional response surface plots for particle size are presented in Figure 6.8 A and B. Higher zeta potential value was obtained with the optimal conditions which were same for obtaining lesser particle size and optimum PDI.

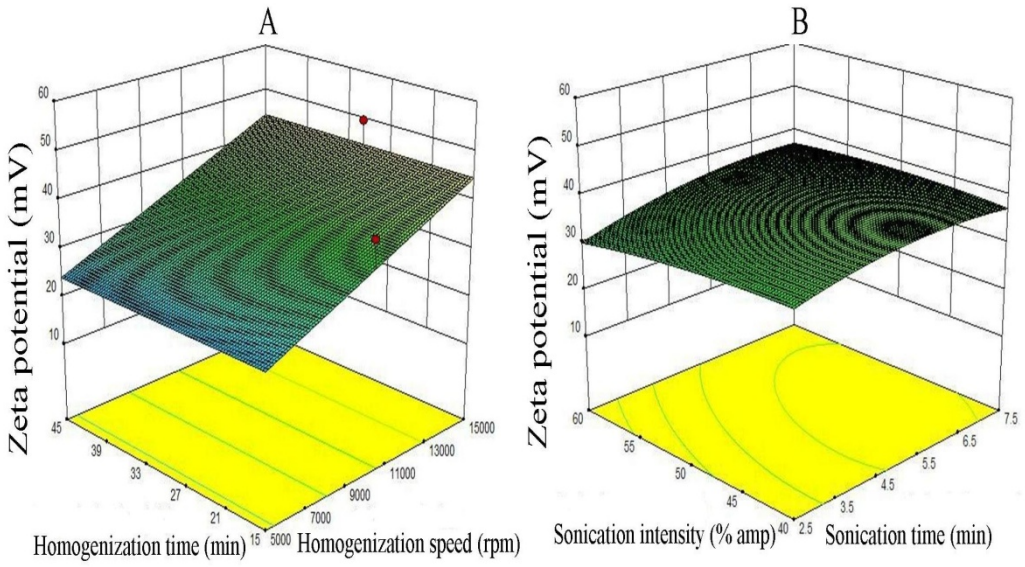

Figure 6.8. 3D images of A - effect of homogenization speed and time on zeta potential and B - effect of sonication time and intensity on zeta potential.

6.3.3.5.Optimization and validation of processing parameters

Optimization of *Ficus religiosa L.* extract loaded SLN was based on combined properties of lesser particle size, lesser PDI and higher zeta potential. From the results, optimum conditions of the processing parameters were set at 15,000 rpm homogenization speed, 30 minutes homogenization time, 5 minutes sonication time and 50 % sonication amplitude.

6.3.4. Preparation and characterization of optimized batch

With these optimized conditions, an optimized SLN batch was prepared by using glyceryl monostearate as lipid at 2 % concentration, combination of poloxamer 188 and sodium deoxycholate mixture in the ration of 25:75 was used as surfactant and 15,000 rpm homogenization speed, 30 minutes homogenization time, 5 minutes sonication time and 50 % sonication amplitude were used as processing parameters.

Optimized batch had 180 nm mean particle size, 0.317 PDI and 57.31 mV zeta potential. Optimized batch was further characterized for surface morphology, *in vitro* release and kinetics. Optimized batch had entrapment efficiency of 54.13 % of lupeol. *In vitro* release studies of optimized SLN formulation and extract suspension were done by dialysis bag diffusion technique. The release of lupeol from *Ficus religiosa* L. extract suspension was high with 66.78 % in 3 hours whereas from SLN it was 56.37 % (Figure 6.9). A biphasic release pattern was observed with extract SLN formulation that is initial burst release followed by sustained release.

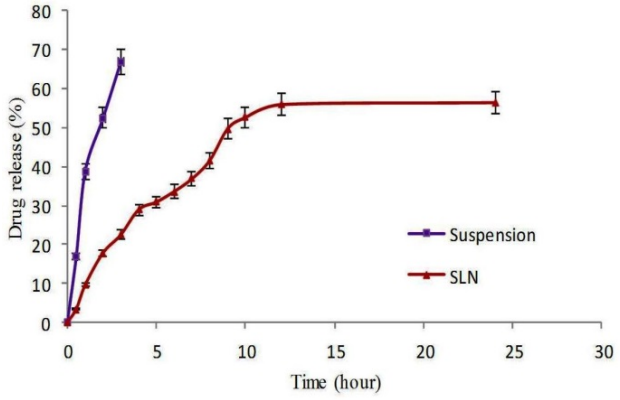

Figure 6.9. *In-vitro* drug release studies of suspension of *Ficus religiosa* L. extract and optimized batch of SLN

After 180 days of storage, there were no significant changes in mean particle size, PDI, zeta potential, and % EE of optimized formulation which revealed that the optimized formulation was stable over 6 months (Table 6.14).

Table 6.14: Stability studies data

S. No.	Stability parameters	0 day	180 days
1	Particle size (nm)	180 nm ± 32.42	197 nm ± 26.53
2	PDI	0.347 ± 0.004	0.314 ± 0.002
3	Zeta potential (mV)	57.31 ± 1.65	55.47 ± 2.78
4	EE (%)	54.13 ± 1.47	53.67 ± 2.61

Mean ± SD (n=3)

6.3.5. Fourier transform infrared spectroscopy.

FTIR spectra of *Ficus religiosa* L. extract, glyceryl monostearate, compritol ATO 888 and SLNs are shown in Figure 6.10. *Ficus religiosa* L. extract showed characteristic peaks at 3398 (O-H stretching), 2926 and 1383 (C-O bond vibrations), (C-H stretching), 1629 (-C=C- vibration), 1157 (C-N stretching) and898 (-C=C-H stretching). All these peaks are characteristic peaks of lupeol and all were present in *Ficus religiosa* L. extract loaded SLN and there was no absence of any functional peaks in all the spectra. Thus, it revealed that there was no significant physicochemical interaction between drug and lipid.

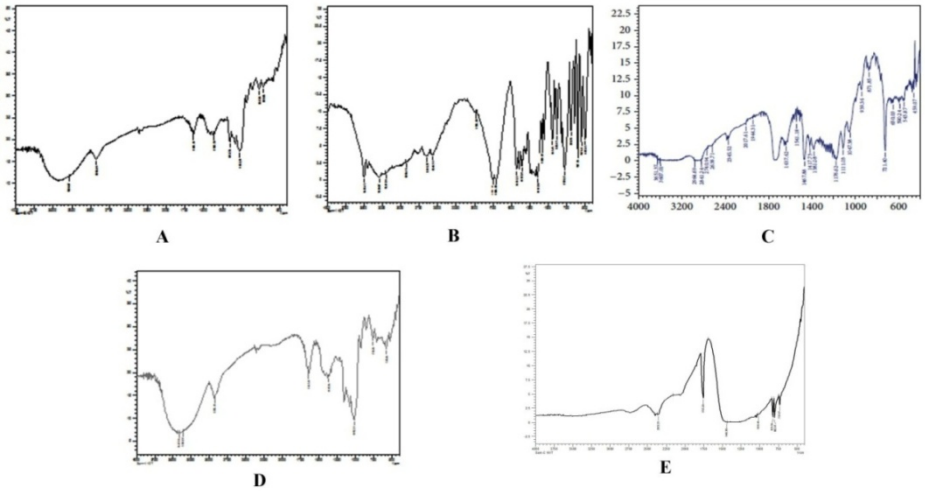

Figure 6.10. FTIR spectra: A - *Ficus religiosa* L. Extract, B – Glyceryl monostearate, C – Compritol ATO 888, D – SLN prepared using glyceryl monostearate and E – SLN prepared using compritol ATO 888

6.3.6. Differential scanning calorimetry

DSC studies revealed that in the thermograms of SLNs (using both lipids), *Ficus religiosa* L. extract peak was reduced and broadened but no change was observed in the lipid peak (Figure 6.11). The broadening of *Ficus religiosa* L. extract peak in nanoparticles might be due to conversion of crystalline form to amorphous form.

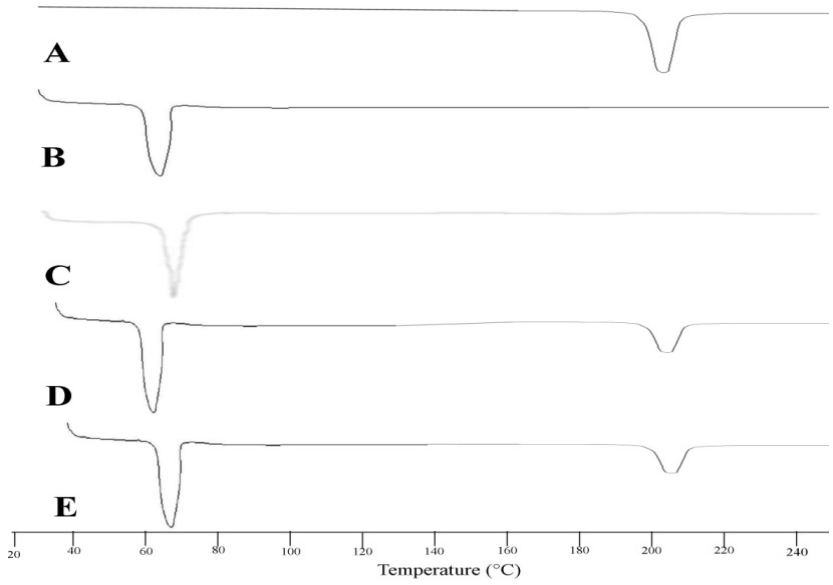

Figure 6.11. DSC thermograms of A - *Ficus religiosa* L. extract, B – Glyceryl monostearate, C – Compritol ATO 888, D –SLN prepared using glyceryl monostearate and E – SLN prepared using compritol ATO 888

6.3.7. **Powder X-ray diffractometry**

PXRD spectra of *Ficus religiosa* L. extract, glyceryl monostearate, compritol ATO 888 and SLNs are shown in Figure 6.12. The diffraction spectrum of *Ficus religiosa* L. extract showed characteristic peaks at 2θ of 13.64, 14.74, 15.97, 19.37, 21.20, 21.57, 22.90, and 24.32 indicating crystalline nature of the *Ficus religiosa* L. extract. The crystalline peaks of *Ficus religiosa* L. extract were absent in SLN formulations indicating that the *Ficus religiosa* L. extract was not in crystalline form. Intensity of lipid peaks (glyceryl monostearate and compritol ATO 888) was also decreased in the SLN formulation. This reduced intensity confirms the decreased crystallinity of lipids in SLN formulations.

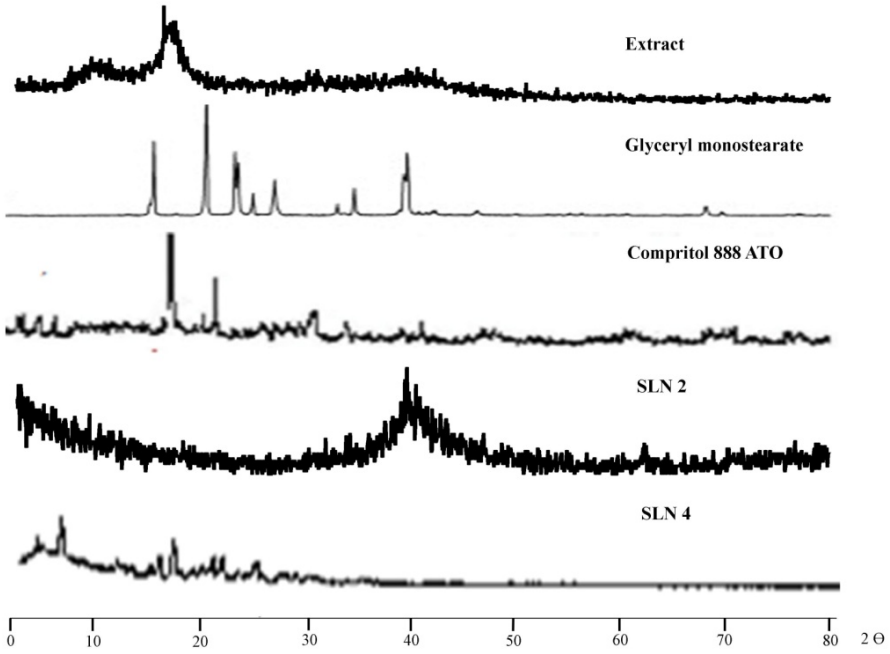

Figure 6.12. PXRD spectra

6.3.8. Preparation and characterization of quantum dots incorporated nanoparticles

The *in vitro* characterization results of CdSe core quantum dots and CdSe/ZnS core-shell quantum dots are shown in Figure 6.13. The absorption maxima of CdSe core quantum dots (Figure 6.13 A) using UV-Visible spectroscopy in aqueous solution was found to be 543 nm and in case of CdSe/ZnS core-shell quantum dots, a smaller shift to longer wavelength was observed which shows the shell formation of ZnS over CdSe core. FTIR analysis of core CdSe quantum dots showed peaks corresponding to cadmium selenide at 3320 cm^{-1} (-OH vibration), 3200 cm^{-1} (-CH vibration), 1750 cm^{-1} (-CO vibration) as shown in Figure 6.13 B whereas in case of CdSe/ZnS core shell quantum dots, termination of carboxyl group was observed which could be attributed to the formation of ZnS shell over CdSe core. PXRD pattern (Figure 6.13 C) of CdSe core quantum dot showed broad peaks at 29.9°, 51.6° and 56.3° which are characteristic peaks

of CdSe whereas in case of CdSe/ZnS core-shell quantum dots, there was a reduction in crystalline peaks of ZnS. This further confirms the shell formation of ZnS over CdSe core. These results are in agreement with the reported data (Wankhede et al. 2008).

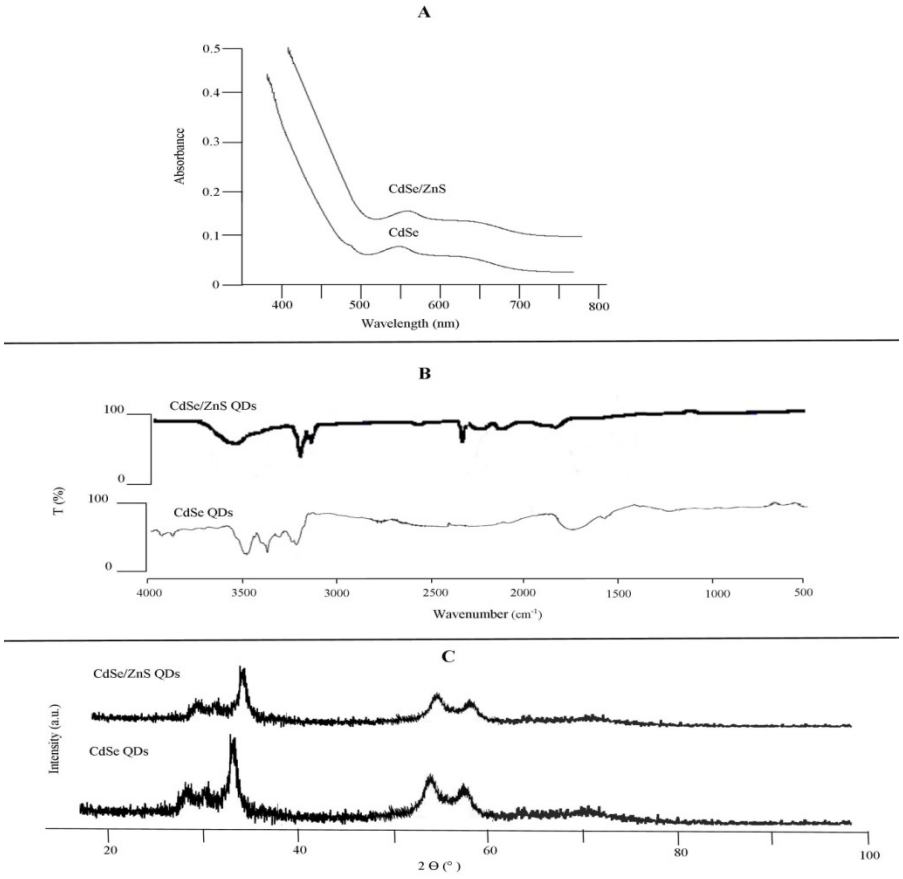

Figure 6.13: Characterization of core CdSe quantum dots; A) UV - Visible absorption spectrum, B) FTIR spectrum and C) PXRD pattern

6.3.9. *In vitro* characterization of targeted and untargeted nanoparticles

There was a slight increase in particle size and PDI of ETNPs than EUNPs (Table 6.15). Also, there was a significant difference in zeta potential of EUNPs and ETNPs

($p<0.05$). EUNPs had zeta potential value of -30.07 ± 4.5 mV whereas ETNPs had zeta potential value of +53.19 ± 5.0 mV. There was no significant difference in the % entrapment efficiency of nanoparticles (Table 6.15). Surface morphology of ETNPs and EUNPs were observed by SEM (Fig 6.14 B and C, respectively). Surface morphology revealed that the nanoparticles were spherical in shape and the particles had size around 200 nm.

Table 6.15: *In vitro* characterization of nanoparticles

Type of nanoparticles	Particle size (nm)	PDI	Zeta potential (mV)	EE (%)	% Drug loading
ETNPs	236.1 ± 24.3	0.3 ± 0.02	+53.19 ± 5.0	59.1 ± 7.3	12.34 ± 0.78
EUNPs	190.7 ± 57.8	0.3 ± 0.07	-30.07 ± 4.5	58.7 ± 4.9	10.74 ± 1.23

Mean ± SD (n=3)

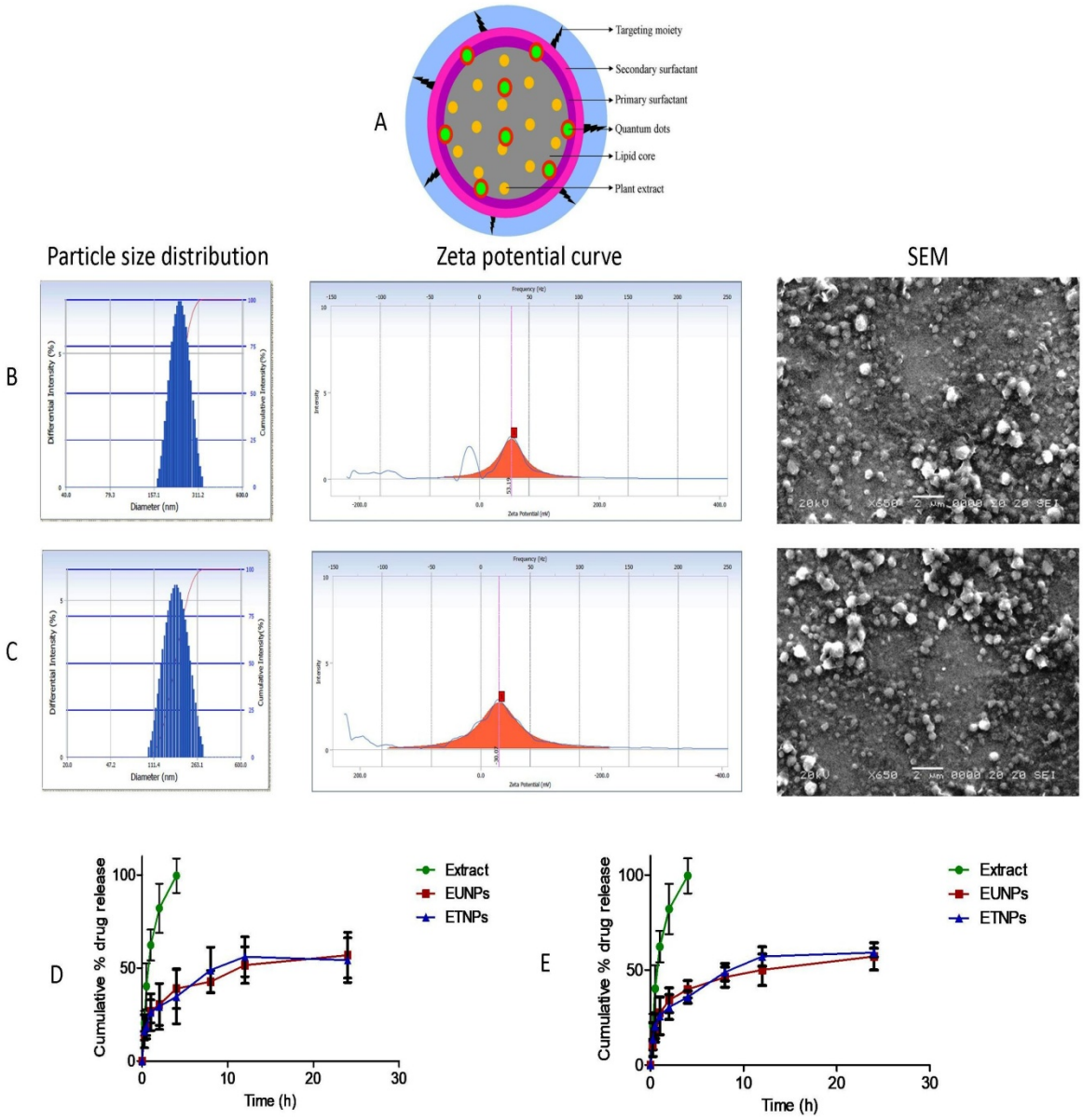

Figure 6.14: *In vitro* characterization of nanoparticles A) diagrammatic representation of ETNPs, B) particle size distribution curve, zeta potential curve and SEM image of ETNPs, C) particle size distribution, zeta potential curve and SEM image of EUNPs, and D) *In vitro* release profiles of *Ficus relgiosa* L. extract, EUNPs and ETNPs in pH 1.2 for first two hours followed by pH 6.8 and E) *In vitro* release profiles of *Ficus relgiosa* L. extract, EUNPs and ETNPs in pH 7.4

As the prepared nanoparticles are intended for oral administration, *in vitro* release studies were carried out in 0.02 M hydrochloric acid, pH 1.2 as release media for first 2 h followed by the use of phosphate buffer, pH 6.8 for the remaining time period. The release of lupeol in pH 1.2 was found to be 63.51 ± 2.45 %, 8.63 ± 1.47 % and 7.87 ± 0.97 % from *Ficus relgiosa* L. extract, EUNPs and ETNPs, respectively. The release of lupeol from *Ficus religiosa* L. extract was high with 96.7 % in 4 h whereas from ETNPs sustained release of lupeol was observed i.e. 56.3 % up to 24 h (Figure 6.14D). No significant difference in the release profile of lupeol from ETNPs and EUNPs was observed ($P>0.05$). *In vitro* release of lupeol from ETNPs and EUNPs followed Higuchi model of release kinetics. Further, the release mechanism was found to be non-fickian model by Korsemeyer–Peppas model (n-values were above 0.4).

After 180 days of storage of ETNPs at 30 ± 2°C temperature and 65 ± 5% relative humidity, there were no significant changes in mean particle size, PDI, zeta potential, and % EE of ETNPs which revealed that the ETNPs were stable over 6 months (Table 6.16).

Table 6.16: Change in particle size, PDI, zeta potential and entrapment efficiency following the storage for 180 days at30 ± 2°C temperature and 65 ± 5% relative humidity

S. No.	Stability parameters	0 day	180 days
1	Particle size (nm)	236.7 ± 63.4	241.6 ± 57.1
2	PDI	0.3 ± 0.02	0.3 ± 0.02
3	Zeta potential (mV)	57.3 ± 7.6	55.4 ± 9.7
4	Entrapment efficiency (%)	59.1 ± 7.3	54.1± 4.2
5	Drug loading (%)	12.34 ± 0.78	11.99 ± 1.2

6.3.10. *In vitro* cytotoxicity assessment

The use of extract as a herbal medicine is expected to have low or no toxicity which is reflected in the results that% cell viability of control is 93.42 % and extract treated group is 91.97 % which is not significantly different from the control group ($p > 0.05$). In spite of the higher cell viability of the extract treated group, excipients used in the nanoformulation might result in cytotoxicity. In order to assess the *in vitro* cytotoxicity of nanoformulations, cells were treated with blank nanoparticles, EUNPs and ETNPs, separately. Percentage cell viability of ETNPs (85.0%), EUNPs (88.5%) or blank nanoparticles (85.4%) showed no significant difference ($p > 0.05$) as compared to control (Figure 6.15 A). This supports that ETNPs prepared using TPP as a mitochondrial targeting moiety, are safe to use.

In addition to this, *in vitro* cytotoxicity of triphenyphosphonium (TPP), at different concentrations (0.125, 0.25, 0.5, 1 and 2 µmol) was studied. The cell viability of TPP treated cells was dependent on the TPP concentration (Figure 15 B), 2 µmol concentration of TPP showed the lowest % cell viability and 0.125 µmol concentration showed highest % cell viability. In all the tested concentrations of TPP, % cell viability was above 80 % which shows that TPP even at 2 µmol concentration is nontoxic *in vitro.*

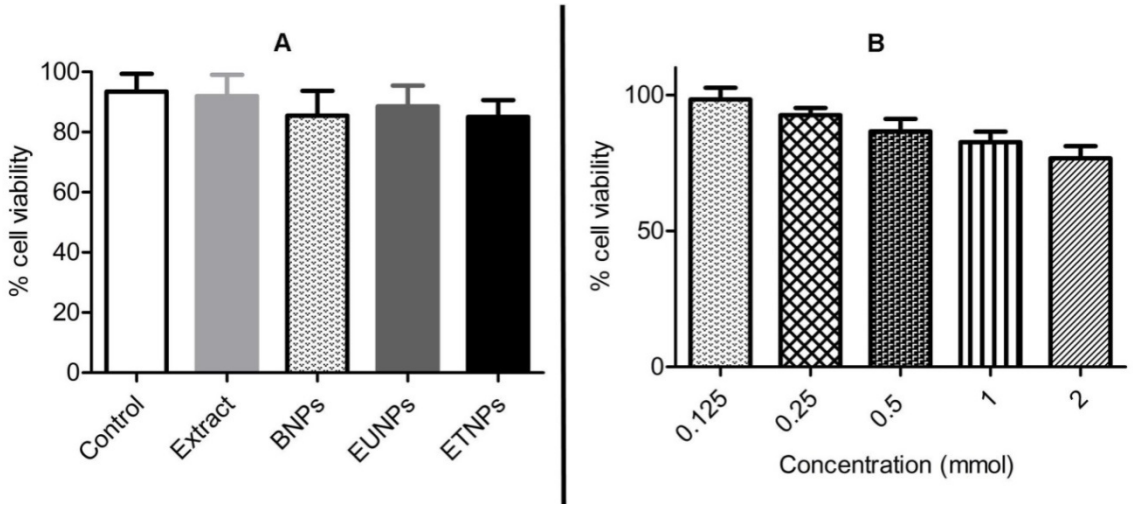

Figure 6.15: *In vitro* cytotoxicity assessments A) different treatment groups and B) different concentrations of TPP

6.3.11. Colocalization by confocal microscopy*in vitro*

To check the targeting ability of nanoparticles to mitochondria, colocalization analysis was performed by staining mitochondria with rhodamine 123. Rhodamine 123 used for staining mitochondria emitted green fluorescence and the CdSe/ZnS quantum dots incorporated into nanoparticles emitted red fluorescence (Figure 6.16). MIN 6 cells treated with EUNPs (4 hours incubation) did not emit red fluorescence for nanoparticles uptake by mitochondria whereas cells treated with ETNPs emitted red fluorescence for nanoparticles uptake by mitochondria.

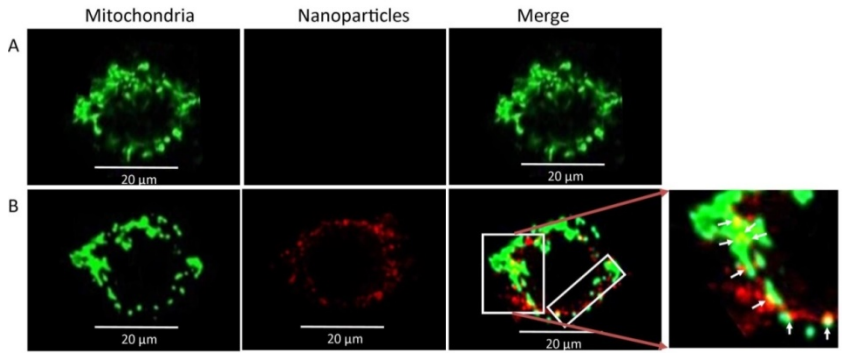

Figure 6.16: Confocal images for colocalization of nanoparticles with mitochondria;A) EUNPs and B) ETNPs

6.3.11. In vivo results

6.3.11.1.Mitochondrial morphology

The shape of mitochondria varies between long tubular to short circular ones (Palade 1952). The shape of mitochondria is maintained by a dynamic balance between fission and fusion processes (Youle and Bliek, 2012). In case of diabetes, mitochondrial morphology will be affected by lack of mitochondrial proteins responsible for fission and fusion process which causes mitochondrial dysfunction (Cipolat et al. 2004).The changes in mitochondrial morphology in diabetic and different treatment groups were studied and compared with control (non-diabetic) group. For clear understanding of structural changes in mitochondria, single mitochondrion was captured (Figure 6.17). In the control group, mitochondrion seems to be in oval shape and the fluorescence emitted by dye (Mitoview 720 for staining mitochondria) was able to view the mitochondrion shape under fluorescence microscopy. In case of diabetes or extract treated group, the sizes of mitochondria seem to be small as compared to control and the shapes of mitochondria were in spherical in both diabetic and extract treated groups whereas ETNPs treated group had the similar morphology to control. EUNPs treated group showed similar

mitochondrion morphology to control but the fluorescence intensity was less than ETNPs or control. The images were captured on average basis.

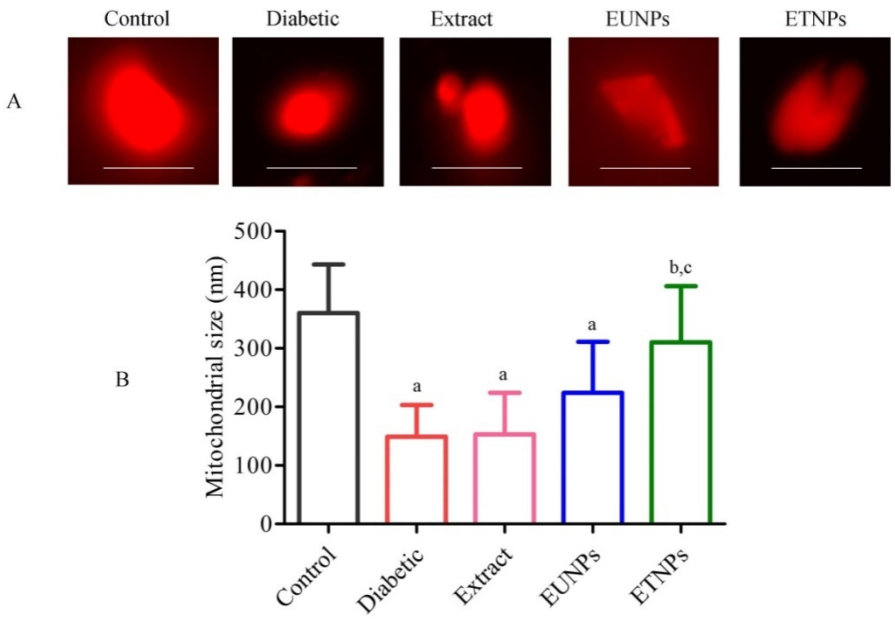

Figure 6.17: Mitochondrial structural changes in A) representative mitochondrial images for size and shape followed by different treatments; JC-1 was used for staining mitochondria and B) histogram representing the size of mitochondria in different treatment groups

Results are expressed as mean ± SEM (n=6) $^{a}P<$ 0.05 compared to normal group; $^{b}P<$ 0.05 compared to diabetic group; and $^{c}P<$ 0.05 compared to *Ficus religiosa L.* extract (one-way ANOVA followed by Tukey's multiple comparison test).

6.3.11.2.Mitochondrial membrane potential

Mitochondrial depolarization during oxidative stress of type 2 diabetes causes release of cytochrome-c into cytoplasm which eventually causes cell apoptosis (Thomas et al. 2007). Hence, changes in mitochondrial membrane potential were studied

in control, diabetic and different treatment groups. The changes in mitochondrial membrane potential in normal, diabetic and different treatment groups were studied. From the results, it was observed that mitochondrial integrity was lost in diabetic rats than control rats. Mitochondrial integrity was effectively regained in rats treated with ETNPs than EUNPs or extract (Figure 6.18).

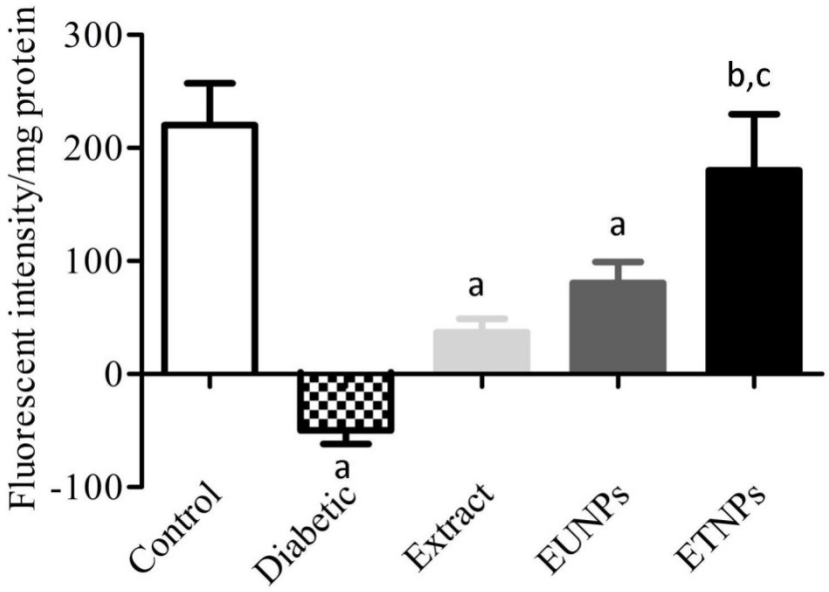

Figure 6.18: Mitochondrial membrane potential of different treatment groups

Results are expressed as mean ± SEM (n=6) [a]P< 0.05 compared to normal group; [b]P< 0.05 compared to diabetic group; [c]P< 0.05 compared to *Ficus religiosa L.* extract; and [d]P< 0.05 compared to EUNPs (one-way ANOVA followed by Tukey's multiple comparison test).

6.3.11.3.Measurement of complex-I, II, IV and V analysis

During diabetes, through the processes of glycolysis and TCA cycle, higher levels of NADH are observed. Hence, more electronic pressure will be imposed on complex I of

ETC by higher levels of NADH which causes complex I dysfunction (Sivitz and Yorek, 2010). When there is impairment in the conventional glycolytic pathway due to higher levels of NADH, glucose will be diverted to polyol pathway. The end product of polyol pathway is NADH, this further increases the NADH level and disturbs complex I activity (Lorenzi 2007). Further, it affects the activity of complex II, IV and V. From the results of complex-I, II, IV and V analysis, it was observed that the complexes activity was significantly ($p<0.05$) reduced in diabetic group. Treatment with extract did not show any effect on complexes activity whereas treatment with EUNPs significantly improved complex I activity but had no effect on complex-II, IV and V. Treatment with ETNPS significantly ($p<0.05$) improved complex-I, II, IV and V activity and it was not significantly ($p >0.05$) different form control group (Figure 6.19). This shows that the targeted delivery to mitochondria using *Ficus religiosa* L. extract improves the decreased activities of complex-I, II, IV and V in diabetic condition.

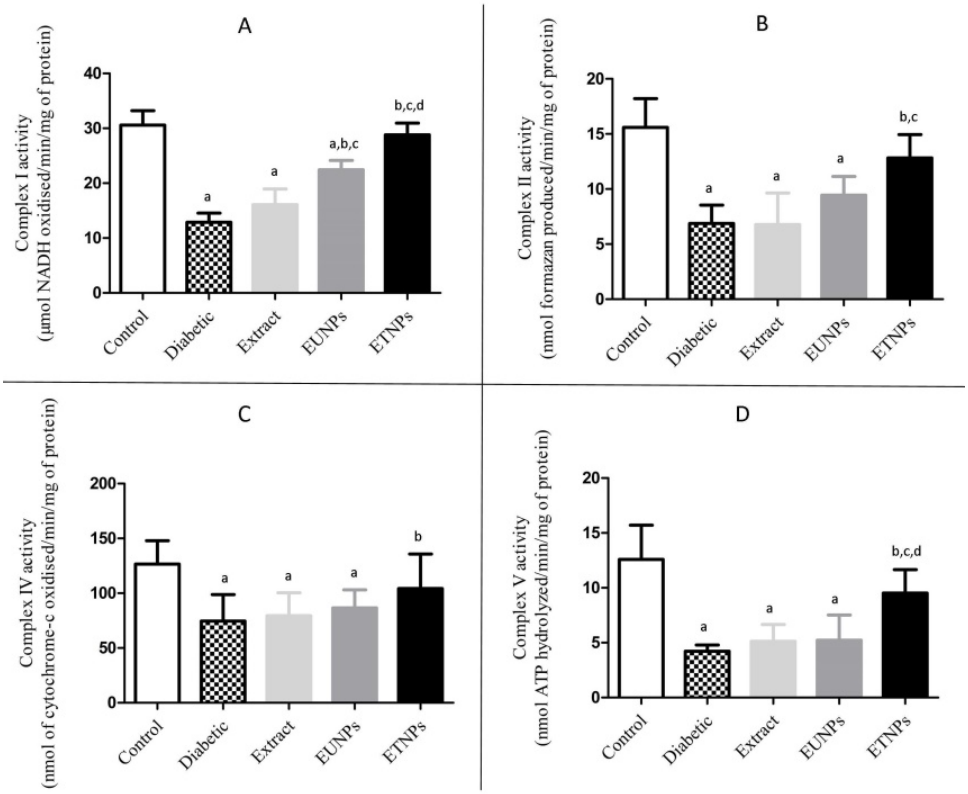

Figure 6.19: Complex-I, II, IV and V activity

Results are expressed as mean ± SEM (n=6) $^{a}P<0.05$ compared to normal group; $^{b}P<0.05$ compared to diabetic group; $^{c}P<0.05$ compared to *Ficus religiosa* L. extract; and $^{d}P<0.05$ compared to EUNPs (one-way ANOVA followed by Tukey's multiple comparison test).

6.3.11.4.Calcium ion concentration

Ca^{2+} present in the mitochondrial matrix and extra mitochondrial locations affects mitochondrial functions. During mitochondrial dysfunction in diabetic condition, increased levels of intracellular Ca^{2+} occurs which induces mitochondrial permeability transition pore and causes release of cytochrome C and finally apoptotic cell death (Hopper et al. 2006).Quantitative analysis of intracellular calcium ion content (Figure 6.20.) revealed significant increase in calcium ion concentration of diabetic group than control group ($p<0.05$). ETNPs treated group significantly reversed calcium ion concentration ($p<0.05$) as compared to EUNPs and extract treated groups ($p>0.05$).

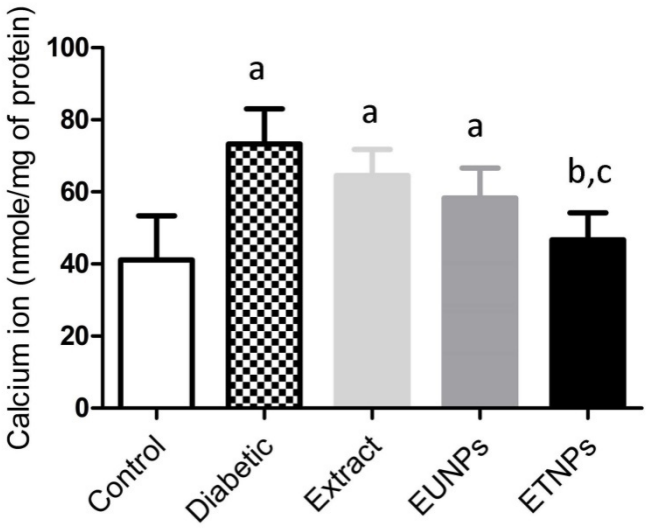

Figure 6.20.: Quantitation of calcium ion concentration in different treatment groups.

Results are expressed as mean ± SEM (n=6) $^{a}P< 0.05$ compared to normal group; $^{b}P< 0.05$ compared to diabetic group; $^{c}P< 0.05$ compared to *Ficus religiosa* L. extract; and $^{d}P< 0.05$ compared to EUNPs (one-way ANOVA followed by Tukey's multiple comparison test).

6.3.11.5.Western blotting

Cytochrome C is a member of complexes involved in electron transport chain of mitochondria and it transfers electron from complex III to IV. During oxidative stress, the high redox potential of cytochrome C, +260 mV reduces to – 400 mV and thus acts as a programmed cell death inducer. This causes release of cytochrome C from mitochondria to cytoplasm and inhibits cascade of caspases. Caspase-3 and caspase-9 are apoptotic markers observed in the oxidative stress of diabetes (Allen et al. 2005). In this study, the apoptotic makers such as cytochrome C, caspase-3 and caspase-9 were studied (Figure 6.21). All three markers expressions were high in diabetic condition and extract and EUNPs treated group showed no significant (p>0.05) difference in expression of these

markers as compared to diabetes. But significant ($p<0.05$) difference in the expression of these markers was observed in ETNPs treated groups.

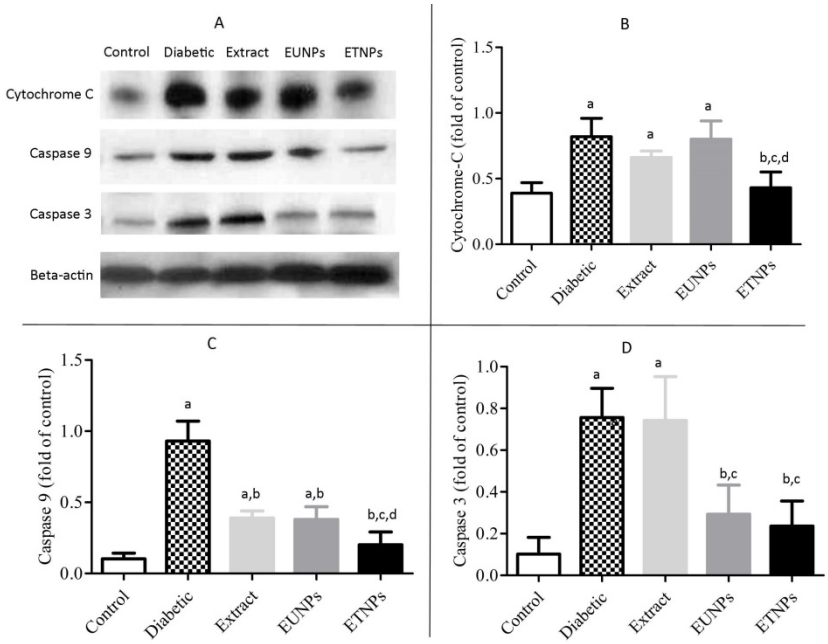

Figure 6.21.: A) Western blotting expressions of cytochrome C, caspase-9 and caspase-3, B) intensity of cytochrome C) intensity of caspase-9 and intensity of caspase-3

Results are expressed as mean ± SEM (n=6) $^{a}P< 0.05$ compared to normal group; $^{b}P< 0.05$ compared to diabetic group; $^{c}P< 0.05$ compared to *Ficus religiosa L.* extract; and $^{d}P< 0.05$ compared to EUNPs (one-way ANOVA followed by Tukey's multiple comparison test).

6.3.11.6.ROS levels estimation

ROS generation in different treatment groups was estimated by using 2',7'-dichlorefluorescein diacetate (DCFDA) as a scavenger. In presence of ROS, DCFDA is oxidized and results in the formation of a fluorescent compound 2',7'-dichlorefluorescein (DCF). The fluorescent intensity of DCF is directly proportion

to the amount of ROS produced. From the results (Figure 6.22), it was observed that higher generation of ROS in diabetic group as compared to control and the extract or EUNPs had no significant ($p>0.05$) effect on reduction in ROS generation. However, ETNPs treatment had significant ($p<0.05$) effect in reducing the ROS generation and this could be due to targeted delivery of an antioxidant extract, *Ficus religiosa* L. extract to mitochondria.

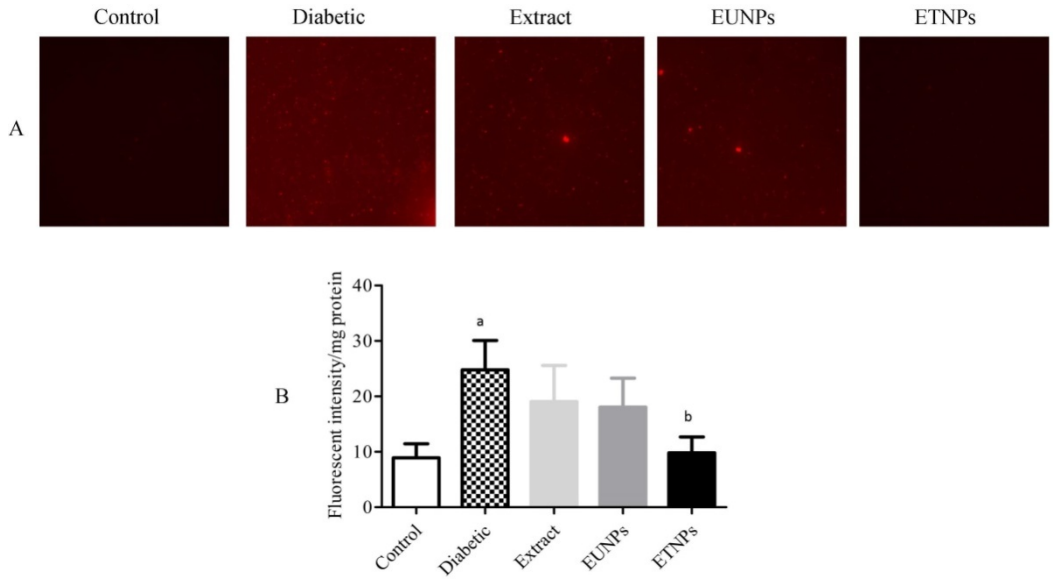

Figure 6.22: ROS generation in different groups and B) corresponding fluorescent intensity of ROS generation in different treatment groups

Results are expressed as mean ± SEM (n=6) $^{a}P< 0.05$ compared to normal group; and $^{b}P< 0.05$ compared to diabetic group; (one-way ANOVA followed by Tukey's multiple comparison test).

6.3.11.7.Antioxidant enzyme levels

Due to the oxidative stress, O_2^- formed in the electron transport chain in mitochondria is dismutated enzymatically to H_2O_2 and then to H_2O in the presence of superoxide dismutase. Increased levels of O_2^- cause decreased superoxide dismutase activity by post-translational covalent modifications (nitration, phosphorylation and glycation) of superoxide dismutase (Banerjee and Vats, 2017). Catalase is an antioxidant enzyme which catalyses reduction of hydrogen peroxides to less reactive oxygen and water. Under oxidative stress, decreased activity of catalase was observed due to tyrosyl nitration of catalase (Valko et al. 2007).Glutathione peroxidase is the major defence antioxidant in oxidative stress and it is responsible for reduction of H_2O_2 to water. In the absence of glutathione peroxidase, detoxification of H_2O_2 doesn't happen and accumulation of OH-radicals occurs (Kurutas 2015).

The levels of different antioxidant enzymes such as superoxide dismutase, catalase and glutathione peroxidase were estimated. It was observed that the levels of superoxide dismutase in diabetic rats were significantly decreased ($p>0.05$) as compared to control rats (Figure 6.23 A). Administration of extract did not show any effect on superoxide dismutase level. However, ETNPs significantly increased ($p<0.05$) the superoxide dismutase levels and this reduction was higher than the group treated with EUNPs. Improvement of superoxide dismutase levels in ETNPs administered rats might be due to reduced level of free radicals. Similarly, reduced level of catalase was observed in diabetic rats as compared to control rats. Treatment with ETNPs reversed the catalase levels than EUNPs or extract treated groups (Figure 6.23 B). In line with earlier observations, decreased level of glutathione peroxidase was observed in diabetic rats as compared to control rats (Figure 6.23 C). Treatment with ETNPs significantly reversed

the level of glutathione peroxidase than EUNPs or extract ($p<0.05$) and it could be attributed to the targeted delivery of *Ficus religiosa* L. extract.

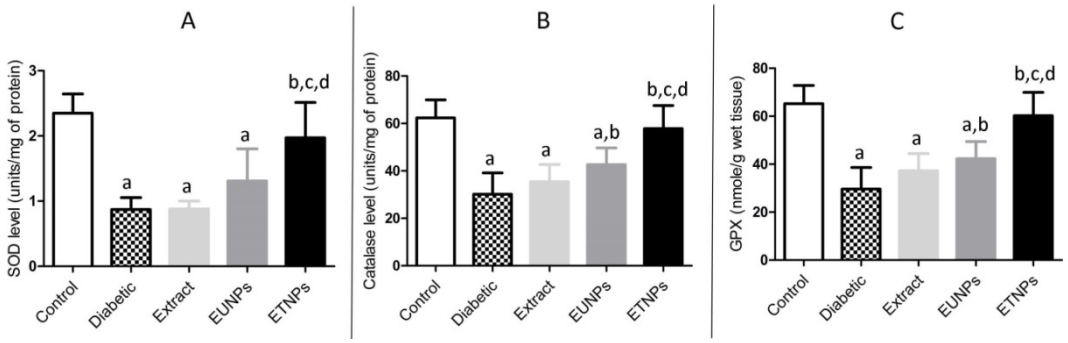

Figure 6.23: Antioxidant levels of different treatment groups on A) superoxide dismutase, B) catalase and C) glutathione peroxidase

Results are expressed as mean ± SEM (n=6) $^{a}P< 0.05$compared to normal group; $^{b}P< 0.05$ compared to diabetic group; $^{c}P< 0.05$ compared to extract and $^{d}P< 0.05$ compared to EUNPs (one-way ANOVA followed by Tukey's multiple comparison test).

6.3.11.8.Nitrite and malondialdehyde levels

Impairment in nitric oxide (NO) production causes endothelial dysfunction which results in the development of insulin resistance and thus, types 2 diabetes mellitus and its associated complications including cardiovascular complications (Sreekumar and Nair, 2007). From the results (Figure 6.24 A), a higher level of nitrite was observed in diabetic rats than the control rats. Treatment with extract or untargeted nanoparticles had no effect on reduction in nitrite levels but treatment with targeted nanoparticles significantly decreased ($p<0.05$) the nitrite level.

Lipid oxidation of free radicals forms a toxic by-product, malondialdehyde. It involves in the cross-linking of glycation products and causes stiffening of cardiovascular

tissue (Youle and Bliek, 2012).Results showed that levels of malondialdehyde formation was significantly higher ($p>0.05$) in diabetic rats than control rats but targeted nanoparticles significantly decreased ($p<0.05$) the levels of malondialdehyde formation than untargeted nanoparticles and extract (Figure 6.24 B).

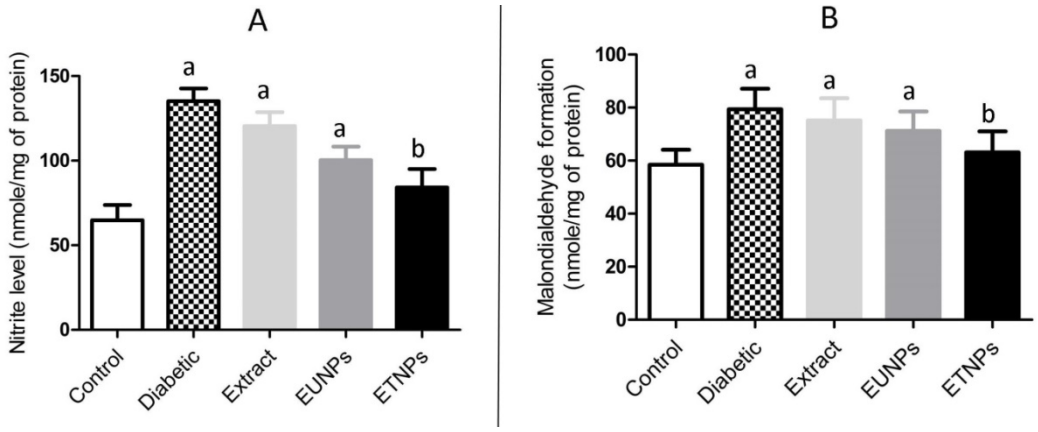

Figure 6.24: Estimation of A) nitrite levels and B) malondialdehyde formation following different treatments

Results are expressed as mean ± SEM (n=6) $^{a}P< 0.05$compared to normal group; $^{b}P< 0.05$ compared to diabetic group; $^{c}P< 0.05$ compared to extract and $^{d}P< 0.05$ compared to EUNPs (one-way ANOVA followed by Tukey's multiple comparison test).

6.3.11.9.**Diabetic markers analyses**

Effect of *Ficus religiosa* L. extract, EUNPs and ETNPs on blood glucose, plasma insulin and serum glycated haemoglobin (HbA1C) levels is shown in Figure 6.25. Results showed increased blood glucose levels in diabetic group than normal group whereas significant reduction ($p<0.05$) in blood glucose level was observed with group treated with ETNPs (Figure 6.25A). The order of glucose reduction by different treatment groups is ETNPs >EUNPs >*Ficus religiosa* L. extract. Plasma insulin level was found to

decrease in diabetic group compared to normal group. Significant improvement ($p<0.05$) in insulin level was effectively achieved by ETNPs than EUNPs or *Ficus religiosa* L. extract (Figure 6.24B). Further, from the results of glycated haemoglobin levels, it was observed that the level of HbA1C was significantly increased in diabetic group compared to control group as shown in Figure 6.25C ($P<0.05$). Treatment with extract or EUNPs did not significantly reduce ($P>0.05$) the HbA1C level whereas treatment with ETNPs significantly reduced HbA1C level ($P<0.05$).

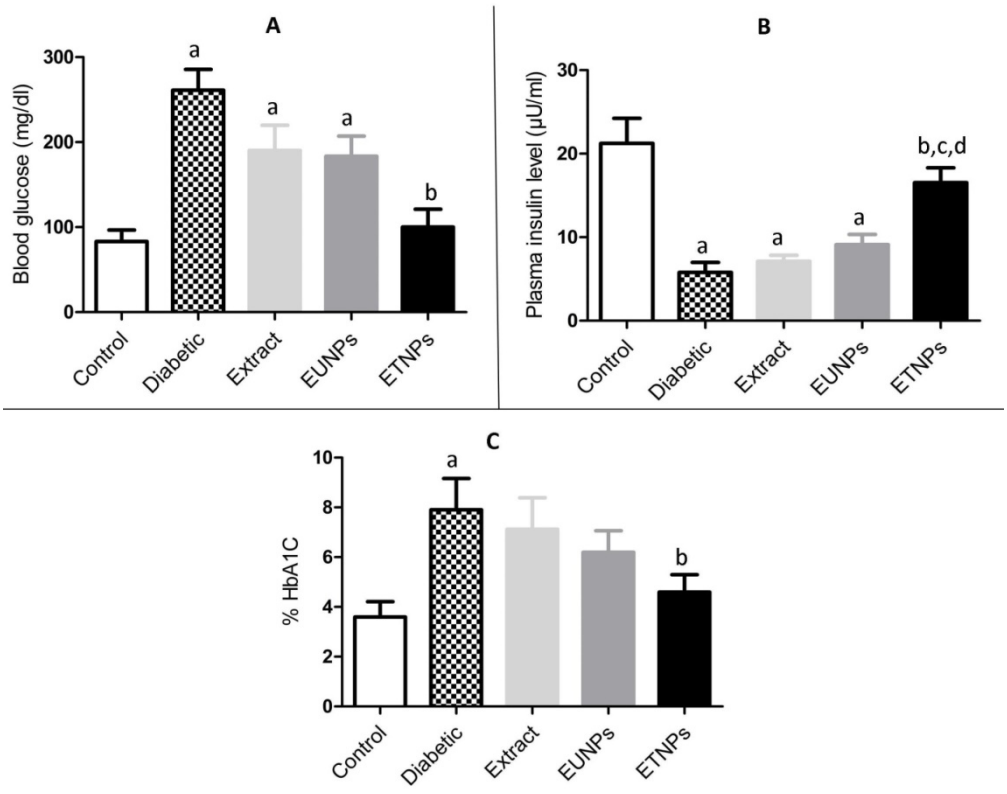

Figure 6.25: Effect of different treatments on A) blood glucose, B) plasma insulin, C) serum glycated haemoglobin

Results are expressed as mean ± SEM (n=6) $^{a}P<0.05$ compared to normal group; $^{b}P<0.05$ compared to diabetic group; $^{c}P<0.05$ compared to extract and $^{d}P<0.05$ compared to EUNPs (one-way ANOVA followed by Tukey's multiple comparison test).

6.3.11.10. Histopathology studies

6.3.11.10.1. Pancreas

In the histopathology of control group of pancreas, normal pancreatic islet cell with normal cell borders. In case of diabetic group, severe degeneration of pancreatic islets including hypochromatosis and disappearance of cell border were observed (Figure 6.26). Treatment with extract did not improve the severe degeneration of pancreatic islets whereas treatment with targeted nanoparticles and untargeted nanoparticles improved the structural integrity of pancreatic islets but the targeted nanoparticles treated group showed similar islet morphology as that of control group.

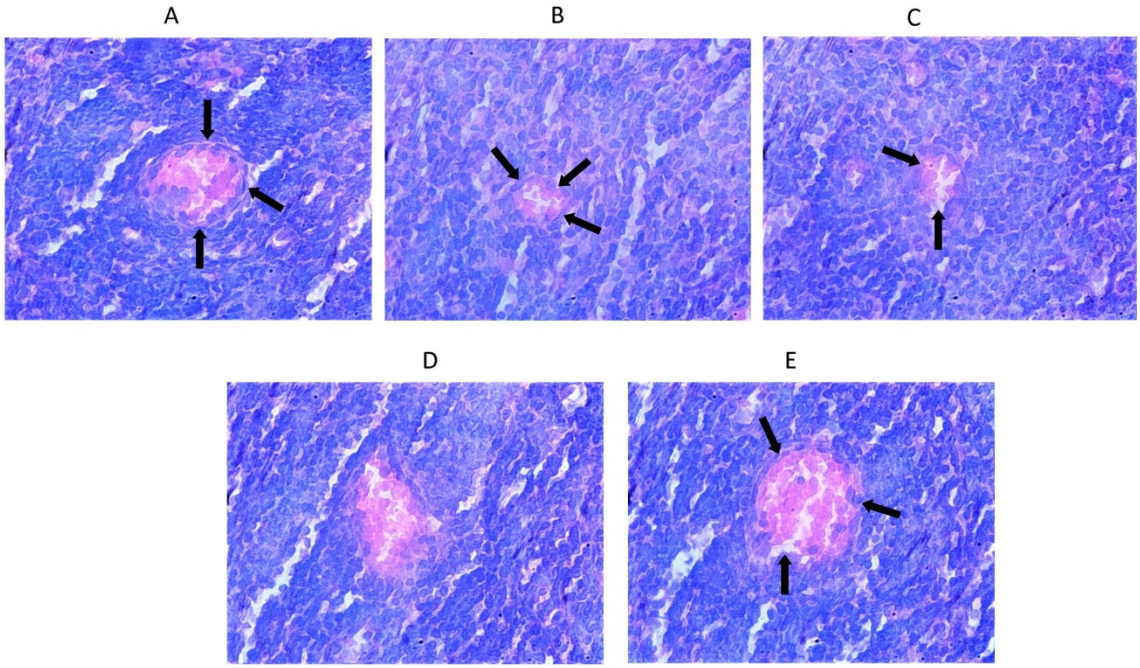

Figure 6.26: Histology examination of pancreas followed by different treatments A) control rat, B) diabetic, C) extract, D) EUNPs and E) ETNPs

6.3.11.10.2. Liver

Histopathology of liver in control group revealed that hepatic cells were arranged in a regular manner along with normal cell borders, further, abundant cytoplasm and central nuclei were observed. In case of diabetic group, disappearance of hepatic cells, fatty degeneration and hypochromatosis were observed which shows hepatic damage in case of diabetes. Treatment with targeted nanoparticles showed improved hepatic cellular morphology whereas untargeted nanoparticles extract had no effect (Figure 6.27).

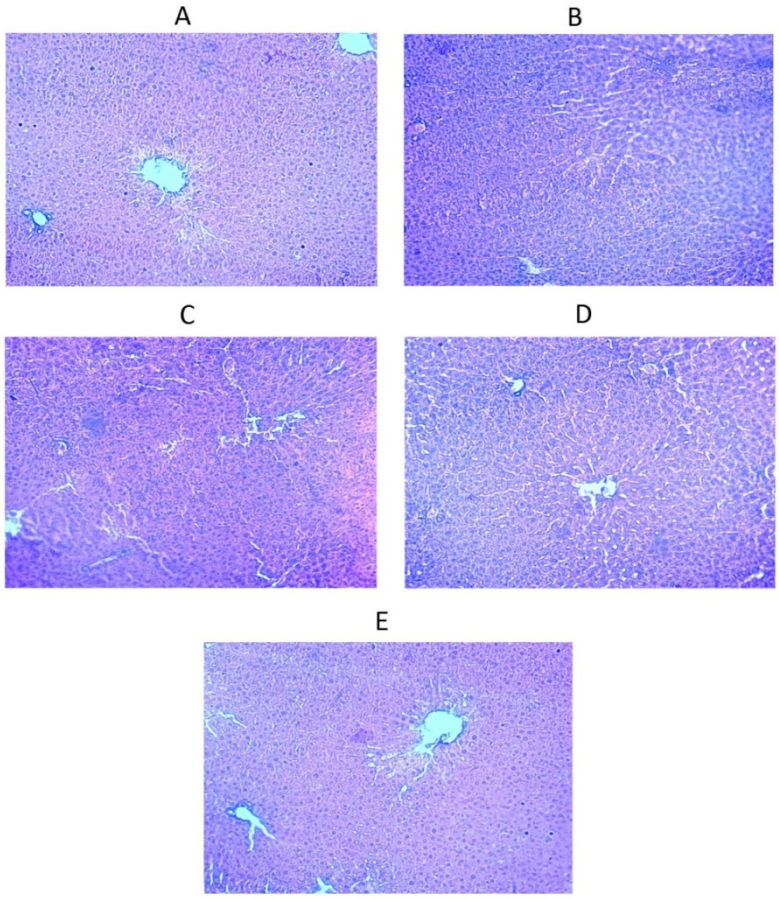

Figure 6.27: Histology examination of liver followed by different treatments A) control rat, B) diabetic, C) extract, D) EUNPs and E) ETNPs

6.3.11.10.3. Skeletal muscle

Skeletal muscle of normal rat showed uniform cells and the cells were located inside the muscle membrane with regular wide gaps whereas diabetic rat showed irregular wide gaps of cells and the degeneration of cells was obvious, this was same in case of extract or EUNPs treated rats. Treatment with ETNPs showed uniform cells located inside muscle membrane with regular wide gaps (Figure 6.28).

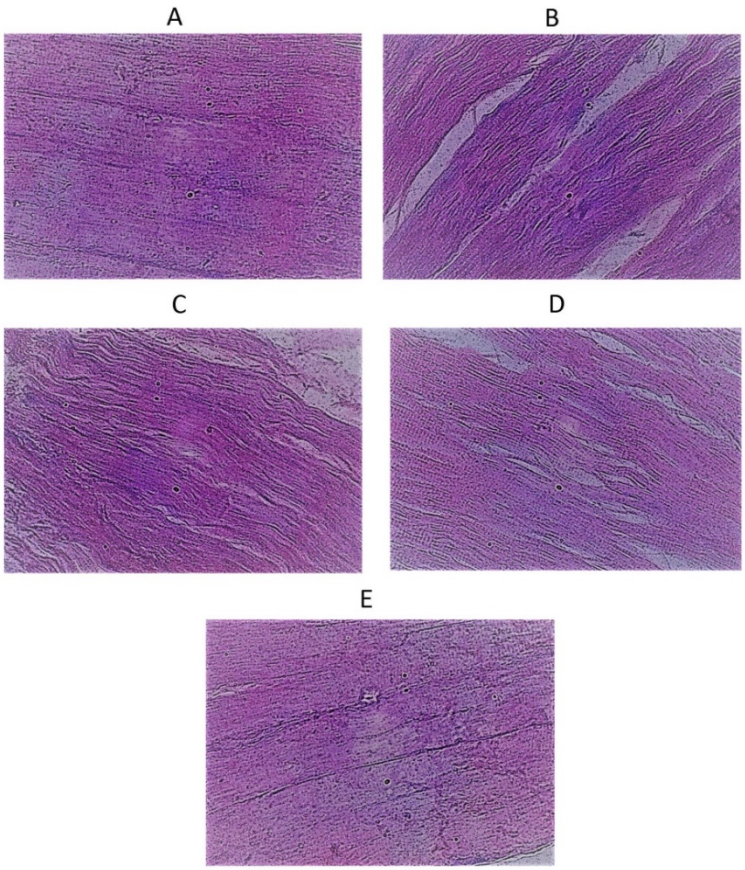

Figure 6.28.: Histology examination of skeletal muscle followed by different treatments A) control rat, B) diabetic, C) extract, D) EUNPs and E) ETNPs

6.3.11.10.4. Adipose tissue

From the results of histopathology of adipose tissue in normal rat showed normal cell structure which were arranged in a regular manner and this was similar in case of both EUNPs or ETNPs treated groups whereas diabetic rat or extract treated rat showed wide gap between cells and the cells were arranged in a irregular manner (Figure 6.29).

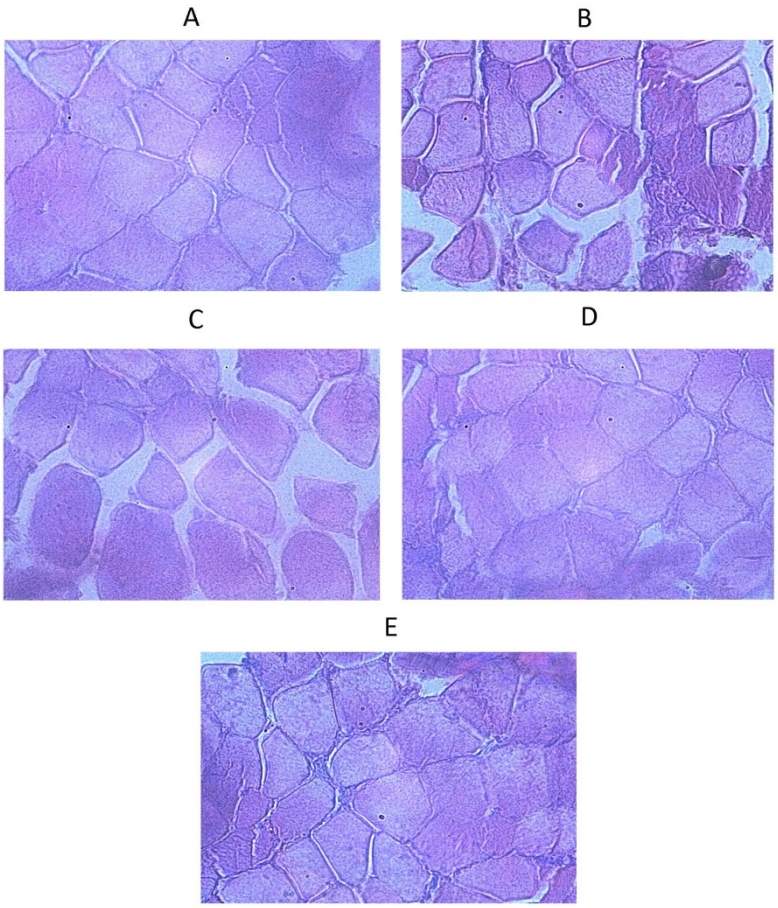

Figure 6.29: Histology examination of adipose tissue followed by different treatments A) control rat, B) diabetic, C) extract, D) EUNPs and E) ETNPs

6.3.11.10.5. Kidney

Photomicrograph of kidney of control rat showed normal structure of glomeruli, tubules whereas diabetic rat showed degenerated glomeruli and tubules with focal necrosis of tubules which was same in case of extract treated group. Kidney of EUNPs treated rat showed regeneration of glomeruli and restoration of tubules and renal cells. ETNPs showed same morphology of glomeruli and tubules as that of control rat (Figure 6.30).

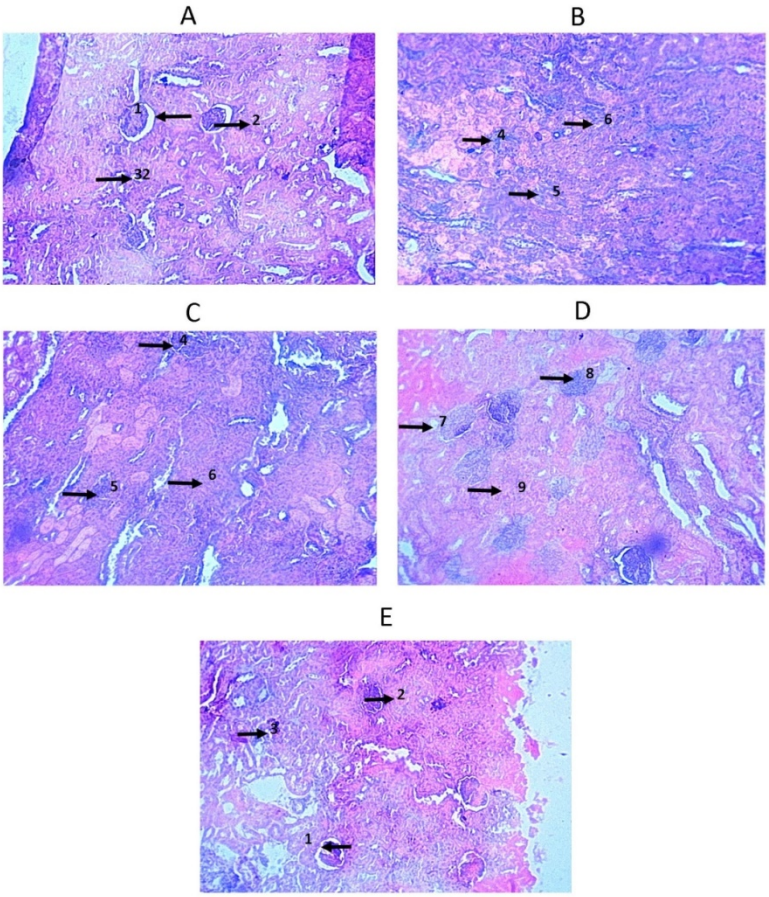

Figure 6.30: Histology examination of kidney followed by different treatments A) control rat, B) diabetic, C) extract, D) EUNPs and E) ETNPs

6.3.11.11. **Pharmacokinetic assessment**

6.3.11.11.1. RP HPLC method development of lupeol in rat plasma

The mobile phase composition of methanol:acetonitrile:water in the ratio of 45:45:10 as optimized for *in vitro* condition (Section 6.1.5.1) was used and it gave better separation with reproducible results with retention time lesser than 10 minutes. The HPLC peak of lupeol standard was free of interfering peaks of plasma at the retention time of 10.3 minutes (Figure 6.31). Linearity was obtained in the concentration range of 20-100 ng/ml with correlation coefficient (r^2) values >0.998. The inter- and intra-day precision of lupeol was within 2 % relative standard deviation (RSD). Accuracy was between 98.24 and 99.15 %. LOD and LOQ for lupeol were found to be 35.90 ng/ml and 81.64 ng/ml, respectively. The extraction efficacies in case of spiked plasma samples were 67 ± 17.4% with RSD values less than 6.2 %.

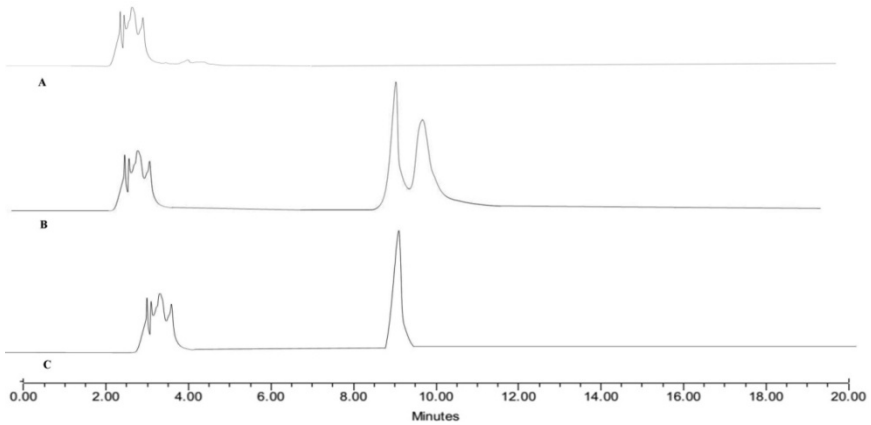

Figure 6.31 . HPLC chromatograms of A – Blank plasma, B – *Ficus religiosa L.* extract, and C – Lupeol standard

6.3.11.11.2. Bioavailability studies

The mean plasma concentration vs. time curve profiles of lupeol from standardized extract suspension and *Ficus religiosa* L. extract loaded SLN are illustrated in Figure 6.32 . Pharmacokinetic parameters of lupeol in *Ficus religiosa* L. extract and SLN formulations are shown in Table 6.17. The mean plasma $AUC_{0–24}$ of lupeol in animals treated with SLN formulation was 9829.83 ± 56.12ng×hr/ml whereas in animals treated with *Ficus religiosa* L. extract suspension, $AUC_{0–24}$ of lupeol was 1068.46 ± 96.4 ng×hr/ml. This increase in $AUC_{0–24}$ for SLN might be due to the avoidance of first pass metabolism by lymphatic transport. The peak plasma concentration (C_{max}) of lupeol in *Ficus religiosa* L. extract suspension was found to be 178.61 ± 24.6 ng/ml and in SLN formulation was found to be 696.57 ± 34.83 ng/ml. Time to reach plasma concentration (t_{max}) in *Ficus religiosa* L. extract suspension was found to be 6 ± 1.1 h and in SLN formulation was found to be 2 ± 0.11 hours. $t_{1/2}$ of lupeol was found to be 7.3 ± 1.0 hours in *Ficus religiosa* L. extract and 15.3 ± 1.3 hours in SLN. From these results, it clearly suggested that the pharmacokinetic profiles of lupeol have been improved in SLN form than *Ficus religiosa* L. extract after oral administration.

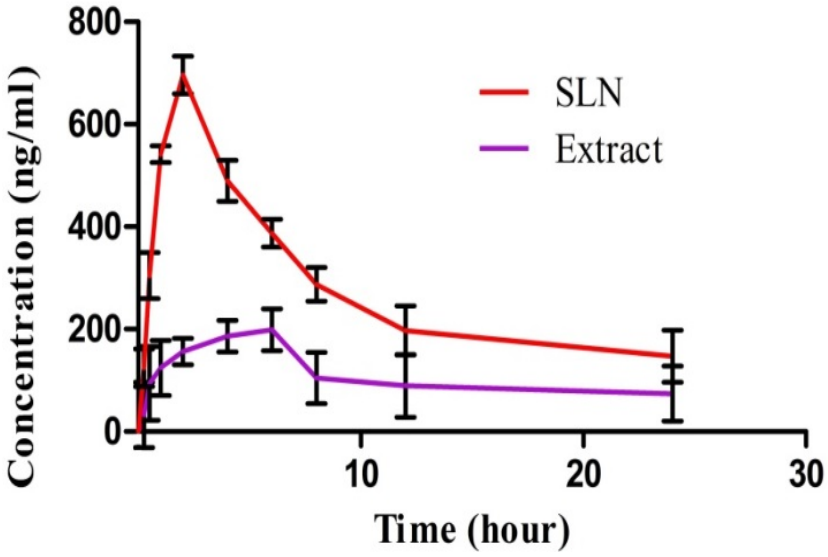

Figure 6.32: Plasma concentration vs. time curve of lupeol in *Ficus religiosa* L. extract suspension and SLN

Table 6.17: Pharmacokinetic parameters of lupeol in *Ficus religiosa* L. in rat plasma

Parameters	*Ficus religiosa L.* extract	SLN
C_{max} (ng/ml)	178.61 ± 24.6	696.57 ± 34.83*
T_{max} (hr)	6 ± 1.1	2 ± 0.11*
AUC_{0-24} (ng×hr/ml)	1068.46 ± 96.4	9829.83 ± 56.12*
$t_{1/2}$ (hr)	7.3 ± 1.0	19.3 ± 1.3*

Mean ± SD; n=6

*p< 0.05, significance difference compared to standardized extract.

The improved pharmacokinetics properties of lupeol in *Ficus religiosa* L. extract loaded SLN might be due to avoidance of enzymatic degradation in the liver. Upon oral administration of *Ficus religiosa* L. extract loaded SLN, they enter lymphatic circulation because of their smaller size and get distributed to body. The lipidic nature of nanoparticles further helps in higher penetration to the cells.

In pancreatic β-cells, the apoptotic mitochondria receive the targeted nanoparticles where nanoparticles release loaded *Ficus religiosa* L. extract (Figure 6.33). The presence of lupeol and other structurally similar compounds in *Ficus religiosa* L. extract possessing both antioxidant and antidiabetic activities may help in neutralization of free radicals with simultaneous hypoglycemic effect.

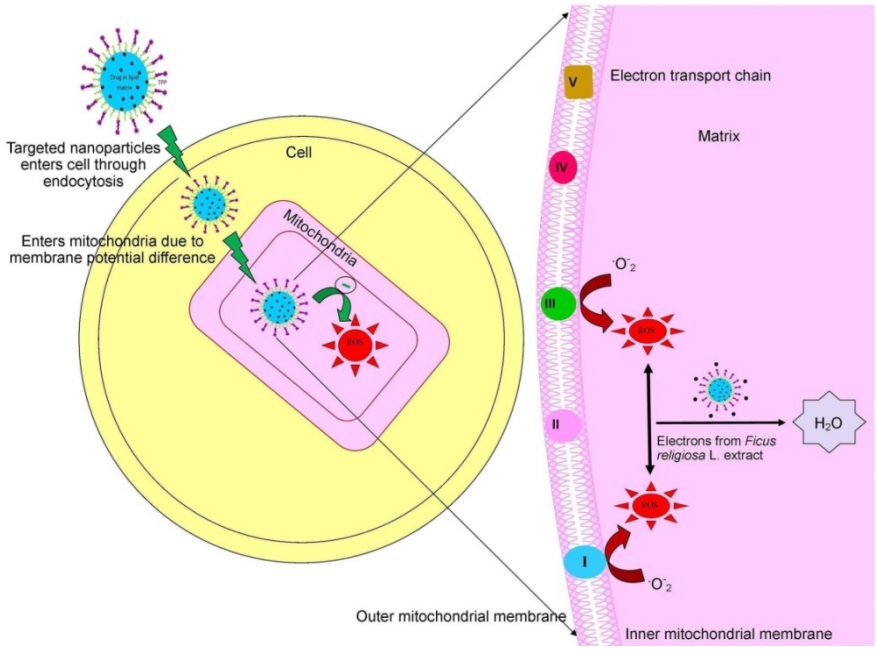

Figure 6.33: Proposed mechanism of action of ETNPs

6.4. Summary

In this study, we report that triphenylphosphonium functionalized *Ficus religiosa* L. extract loaded nanoparticles can target mitochondria and exert their action in oxidative stress induced diabetes. Sustained release of extract from nanoparticles could be attributed to the reduction in dose of *Ficus religiosa* L. extract and reduce frequent drug administration which are most common disadvantages associated with extract. Non-toxic

profile of targeted nanoparticles loaded with *Ficus religiosa* L. extract will be beneficial for chronic treatment of diabetes. Better uptake of targeted nanoparticles by mitochondria proves the targeting ability of nanoparticles to mitochondria. Further, improvement by ETNPs in mitochondrial morphology, calcium ion concentration, complexes, I, II. IV and V activities, antioxidant levels and mitochondrial membrane potential along with reduction in apoptotic markers and ROS level show the improvement of mitochondrial function in the oxidative stress of diabetes. In addition to this, effect of targeted nanoparticles on blood glucose, plasma insulin and HbA1C supports the use of *Ficus religiosa* L. targeted nanoparticles in the management of diabetes. Further, histopathology study reveals that the ETNPs are safe to use in the long term management of diabetes. Pharmacokinetic study revealed the improved bioavailability and extended half-life of lupeol in SLN form.